

Article

Towards Nearly-Zero Energy in Heritage Residential Buildings Retrofitting in Hot, Dry Climates

Hanan S. S. Ibrahim ^{1,2,*}, Ahmed Z. Khan ¹, Yehya Serag ² and Shady Attia ³

¹ Sustainable Architecture and Urbanism Lab, Department of BATir, School of Engineering (EPB), Free University of Brussels/Université Libre de Bruxelles (ULB), 1050 Brussels, Belgium; ahmed.khan@ulb.be

² Department of Architectural Engineering, Faculty of Engineering and Technology, Future University in Egypt (FUE), Cairo 11835, Egypt; yehia.mohamed@fue.edu.eg

³ Sustainable Building Design (SBD) Lab, Department of UEE, Faculty of Applied Sciences, University of Liège, 4000 Liège, Belgium; shady.attia@uliege.be

* Correspondence: hanan.ibrahim@ulb.be

Abstract: Retrofitting “nearly-zero energy” heritage buildings has always been controversial, due to the usual association of the “nearly-zero energy” target with high energy performance and the utilization of renewable energy sources in highly regarded cultural values of heritage buildings. This paper aims to evaluate the potential of turning heritage building stock into a “nearly-zero energy” in hot, dry climates, which has been addressed in only a few studies. Therefore, a four-phase integrated energy retrofitting methodology was proposed and applied to a sample of heritage residential building stock in Egypt along with microscale analysis on buildings. Three reference buildings were selected, representing the most dominant building typologies. The study combines field measurements and observations with energy simulations. In addition, simulation models were created and calibrated based on monitored data in the reference buildings. The results show that the application of hybrid passive and active non-energy generating scenarios significantly impacts energy use in the reference buildings, e.g., where 66.4% of annual electricity use can be saved. Moreover, the application of solar energy sources approximately covers the energy demand in the reference buildings, e.g., where an annual self-consumption of electricity up to 78% and surplus electricity up to 20.4% can be achieved by using photo-voltaic modules. Furthermore, annual natural gas of up to 66.8% can be saved by using two unglazed solar collectors. Lastly, achieving “nearly-zero energy” was possible for the presented case study area. The originality of this work lies in developing and applying an informed retrofitting (nearly-zero energy) guide to be used as a benchmark energy model for buildings that belong to an important historical era. The findings contribute to fill a gap in existing studies of integrating renewable energy sources to achieve “nearly-zero energy” in heritage buildings in hot climates.

Keywords: passive strategies; active strategies; building integrated photovoltaic; BIPV; building integrated solar thermal (BIST); MENA region; Egypt; Khedivial Cairo



Citation: Ibrahim, H.S.S.; Khan, A.Z.; Serag, Y.; Attia, S. Towards Nearly-Zero Energy in Heritage Residential Buildings Retrofitting in Hot, Dry Climates. *Sustainability* **2021**, *13*, 13934. <https://doi.org/10.3390/su132413934>

Academic Editor: Asterios Bakolas

Received: 17 November 2021

Accepted: 14 December 2021

Published: 16 December 2021

Publisher's Note: MDPI stays neutral with regard to jurisdictional claims in published maps and institutional affiliations.



Copyright: © 2021 by the authors. Licensee MDPI, Basel, Switzerland. This article is an open access article distributed under the terms and conditions of the Creative Commons Attribution (CC BY) license (<https://creativecommons.org/licenses/by/4.0/>).

1. Introduction

The net-zero emissions roadmap involves a global energy system transformation by 2050, as stated by the International Energy Agency (IEA) [1]. This roadmap and other global initiatives such as the Climate Action Plan and Paris Agreement pay massive attention to the decarbonisation of the building sector and transition towards a clean energy utilization (e.g., renewable energy sources (RES)) in sector [1–5]. Moreover, integrating the RES in the building sector—more precisely, in existing buildings—is essential to foster maximising energy production on a large scale (e.g., districts and regions) [2,6]. Heritage buildings, which are usually characterized by low energy performance, comprise a large proportion of the existing buildings in many countries in the world [7,8]. Retrofitting

heritage buildings is a complex task where many criteria are weighed against each other, and transiting them towards clean energy utilization needs special attention [2,8]. Accordingly, conservation-compatible energy retrofitting strategies and scenarios that integrate renewable energy resources (RES) utilization in those strategies [9,10] need to be developed. Martínez-Molina et al. (2016) revealed that several energy retrofitting projects and studies in heritage buildings were carried out in cold zones, e.g., the UK and USA, while hot zones, e.g., Libya and Morocco, had few initiatives in this field [11], although climate is an important factor in such contexts since it influences energy use in the achievement of comfort [12]. Accordingly, retrofitting heritage buildings for energy efficiency became a top priority in such severe climates. The Middle East and North Africa (MENA) region, which includes most developing countries, is exposed to various crises such as water and energy shortages, due to rapid climate change in recent decades [13,14]. Additionally, most developing countries in the MENA region face a problem with the demand for appliances and cooling equipment, as around 650 million air conditioners are expected to be added by 2030 [1]. Thus, as stated in the net-zero emissions roadmap, developed countries are closer to achieving net zero emissions than developing ones [1]. In contrast, these countries have great potential for clean energy utilization, due to their exposure to a large amount of solar radiation that promotes installing photovoltaic technology for electricity generation [15–17].

In Egypt—as an example of a developing country located in the MENA region’s hot climate—Cairo has a substantially higher energy consumption than cities in the same climate, as stated by the World Bank [18]. Moreover, almost half of the total annual electricity in Egypt is consumed by the residential sector [19], due to low indoor comfort levels [18,20]. As a result, the growth of electricity demand in Cairo has outpaced economic growth, and it is expected to grow at 5 to 7% per year in the future [18]. For that reason, the Egyptian government issued Ministerial Council Decree no. 1947/2014 and 2532/2016, which set a target to achieve 300 MW of electricity to be generated by solar photovoltaic (PV) that can be installed on buildings’ rooftops [21]. Almost 95 MW of the total electricity generation is expected to be consumed by Cairo only [21]. Cairo possesses more than 688,000 existing buildings and 598,000 of those are residential [22]. Furthermore, Cairo has 3300 heritage buildings and downtown Cairo has 650 listed heritage buildings [22]. Thus, heritage residential buildings need to be retrofitted under an informed energy approach, embracing the concept of nearly-zero energy buildings “nZEBs”, referring to buildings that exhibit high energy performance, requiring the energy used to be generated by renewable resources such as on-site or nearby energy sources [23]. “nZEBs” should be distinguished from net-zero energy buildings, which refers to buildings that use energy generation by RES to cover net energy use, and the buildings can then export or import energy to the grids, based on the quantities of energy required and produced [23].

In summary, there is a need to achieve the lowest possible energy use in heritage residential buildings without altering their aesthetic values in hot climates. This article contributes to fill the gap in this field. Thus, this work is a part of a wider-scale research project comprising a series of published articles [12,24,25]. The research process has multiple stages that start with developing a classification method to select reference buildings of a heritage building stock [24], proposing a retrofitting checklist based on in-depth analysis of cultural values [24,25], and assessing the potential of applying passive retrofitting scenarios to enhance indoor thermal comfort [12]. Lastly, in this article, we assess the potential of transforming the heritage residential building stock towards “nearly-zero energy” and apply the entire methodology developed through the previous stages. Accordingly, this work is presented in five sections. The literature review, the research problems, objectives, and questions have been identified here in the introduction. In Section 2, we explain the research methodology which is introduced in seven subsections. In Section 3, we analyze the results. In Sections 4 and 5, we discuss the study results, implications, and limitations.

1.1. Literature Review

Energy retrofitting of buildings can be fulfilled by many solutions and new technologies, but not every solution can be applied to heritage buildings due to cultural value restraints [26]. Recently, some research has emphasized that passive and active retrofitting actions together with the integration of RES are crucial factors for achieving the lowest possible energy use in heritage buildings in hot climates. For instance, in southern Europe, which has a warm summer [27], specifically in İzmir, Turkey, Şahin et al. (2015) proposed a methodology that integrates passive and active energy retrofitting measures based on a risk–benefit assessment of heritage values [28]. Another study in İzmir, conducted by Güleroğlu et al. (2020), proposed an integrated approach consisting of four phases to examine energy and seismic issues in historical buildings [29]. These studies showed that the highest energy performance can be achieved by applying thermal insulation for the external walls and the replacement of the HVAC system. Another study was carried out in southern Europe, Naples, Italy, by Bellia et al. (2015) in an individual case [30]. The study revealed that there is no need to add insulation materials to the external walls if the walls are thick and heavy [30].

In hot, dry climates, some studies were carried out in non-heritage buildings in the United Arab Emirates (UAE) by Salameh et al. (2020 and 2021) [15–17]. These studies stressed that the utilization of solar energy is more environmentally friendly than other energy sources. The studies also emphasized that the applications of solar energy need lower operating and maintenance costs, and no significant operational pollution is expected [15–17]. Both Lucchi et al. (2020) and Polo Lopez et al. (2020) [10,31] are consistent with the work of Salameh et al. (2020 and 2021) [15–17] in terms of the importance of the integration of RES, i.e., solar energy applications, to cover demand for energy in existing buildings. Additionally, they pointed out that the applications of solar energy (e.g., photovoltaics (PV) and solar thermal (ST)) can be perfectly integrated with the building envelope components of heritage buildings [10,31]. Other similar studies were carried out in non-heritage buildings in Egypt, in a hot, dry climate, such as the work of Attia et al. (2013) and Fahmy et al. (2020) [20,32,33]. Fahmy et al. focused only on analyzing existing studies concerned with urban microclimate and housing typologies and did not tackle specific strategies of the (RES) application in the Egyptian climate. In contrast, the work of Attia et al. (2013) developed an energy simulation tool called ZEBO to help decision makers achieve net-zero energy targets in residential buildings in hot climates, with a case study of Cairo [32]. The study highlighted the importance of combining passive and active strategies to inform decision making for net-zero energy targets in residential buildings in hot climates, more specifically in Egypt [32]. Despite the valuable studies carried out in hot, dry climates, none of them were conducted in heritage residential buildings.

1.2. Research Problems and Objectives

There is a gap regarding integration approaches that reconcile new retrofitting technologies and cultural values to achieve “nearly-zero energy” in heritage residential building stocks in hot, dry climates. Therefore, in this article, we aim to assess the potential of heritage building stock to achieve “nearly-zero energy” in hot, dry climates. Moreover, we also aim at developing an integrated retrofitting approach that balances multi-performance targets in historic districts in such climates. Accordingly, the following questions were asked:

- How can heritage buildings transform to become energy neutral in hot climates?
- What are the optimal scenarios that can achieve the nearly-zero energy target while preserving cultural values?

To find answers to these questions, a methodology based on four phases was proposed. Figure 1 shows a graphical abstract of the proposed methodology. Based on advanced building science and technologies, it is expected that this work will contribute to updating the energy retrofitting policies of heritage buildings not only in Egypt, which has a scarcity or absence of such initiatives, but also in other hot zones. Additionally, it will contribute

to updating both Egyptian energy codes [34,35] and conservation laws (Egyptian Law No. 144 of 2006) [36] to embrace heritage buildings in their context. According to the knowledge of the authors, the presented integrated retrofitting methodology based on a series of validated and tested stages was conducted for the first time in a historic city located in a hot, dry climate such as Cairo, Egypt.

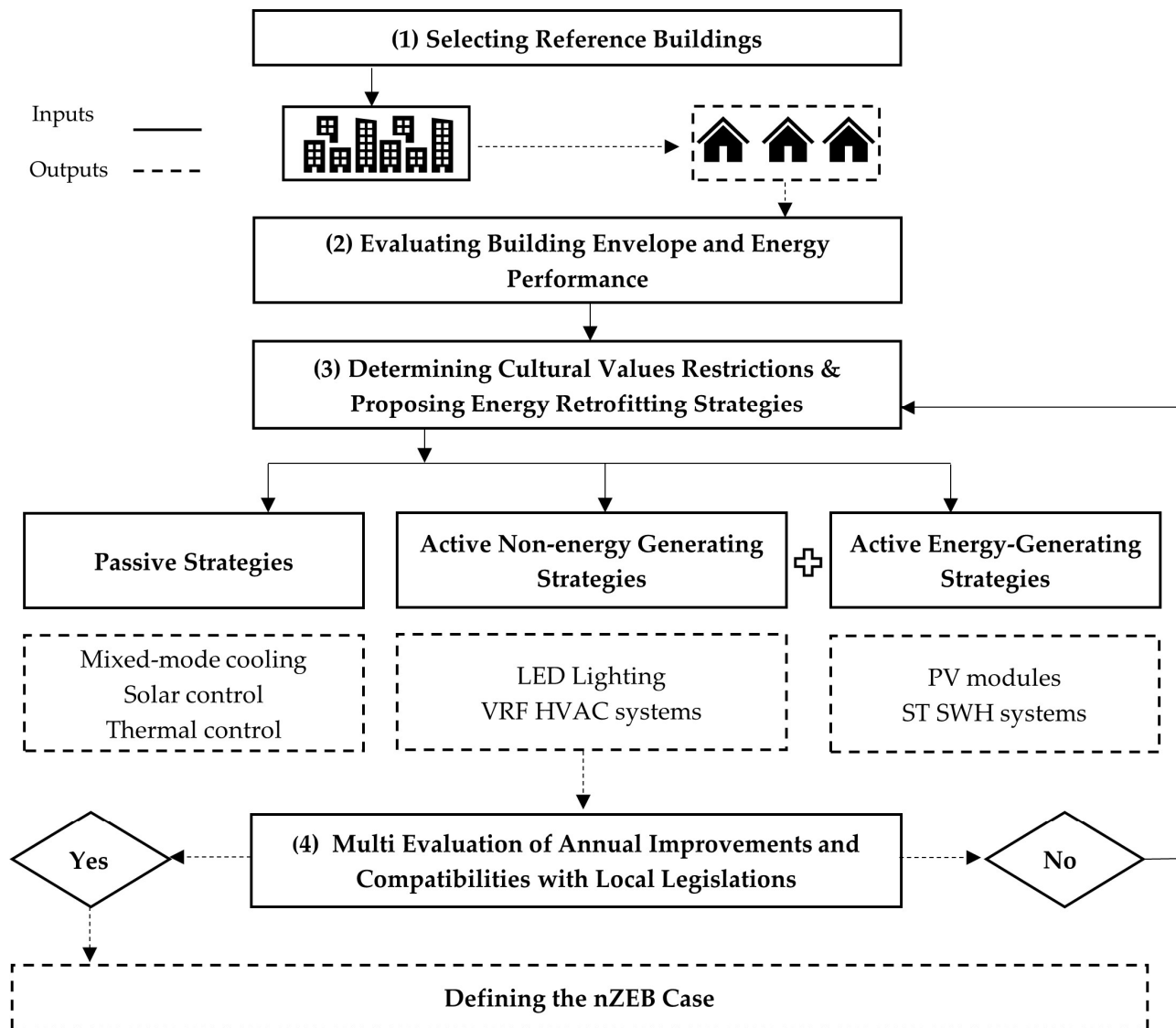


Figure 1. Graphical abstract of the proposed retrofitting methodology.

2. Materials and Methods

The research methodology of this study is summarized and presented in a conceptual framework in Figure 2.

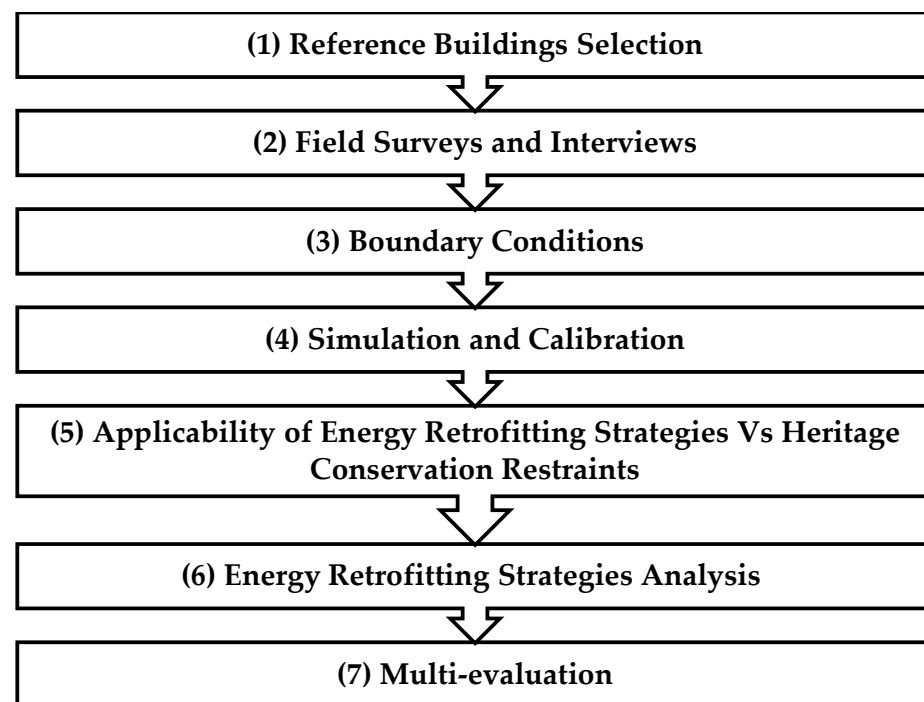


Figure 2. Conceptual framework of this study.

2.1. Reference Buildings Selection

Three heritage residential buildings were selected based on specific criteria, as explained in the following subsection. These buildings are located in downtown Cairo, in the part well known as Khedivial Cairo. This part acts as a ‘buffer zone’ for the UNESCO Heritage Site of ‘Historic Cairo’ [12,24].

2.1.1. Criteria for Selecting Reference Buildings

Two criteria were used to select the case study buildings. The first was based on buildings that represent the largest percentage of the weighted/volume share of the building stock in the study area. Both average values of floor area and building volume in different building typologies were considered. Therefore, based on our most recent publication, entitled “Classification of heritage residential building stock and defining sustainable retrofitting scenarios in Khedivial Cairo”, heritage residential buildings in Khedivial Cairo were classified into twelve classes that represent twelve reference buildings [24]. The classification was based on the number of floors, number of adjoining walls, building construction type, and materials. Accordingly, the twelve reference buildings are listed in a detailed catalogue and numbered from 1 to 12. Moreover, reference buildings that represent the largest building classes of stock were selected. These buildings represent 50.7% of the total building’s volume and equal 133 heritage residential buildings [24]. Another selection criterion was the ability to perform an in-depth investigation inside case study buildings. Because these buildings are inhabited by residential households, field investigation inside these buildings is not often allowed for researchers.

2.1.2. Description of The Selected Reference Buildings

Based on the above-mentioned criteria, three reference buildings were selected as case studies. Figure 3 shows real photos of the selected buildings. Following the work of Ibrahim et al. (2021), the buildings are referred to as reference buildings 7, 8, and 9. The selected buildings are inhabited by middle-income occupants, as labeled by (CAPMAS) [22]. The selected buildings are mixed-mode ventilation buildings that use a mixed ventilation control inside spaces, natural ventilation, and air conditioning (AC). The top floors are the surface area that is most exposed to solar radiation throughout the year, especially in

summer. Thus, a typical apartment on the top floor in each reference building was selected, according to residents' willingness to install data loggers during the survey period. Figure 4 shows typical plans of the selected case study buildings. The occupied areas of the selected apartments are 125, 95, and 110 (m²), of reference buildings 7, 8, and 9, respectively.

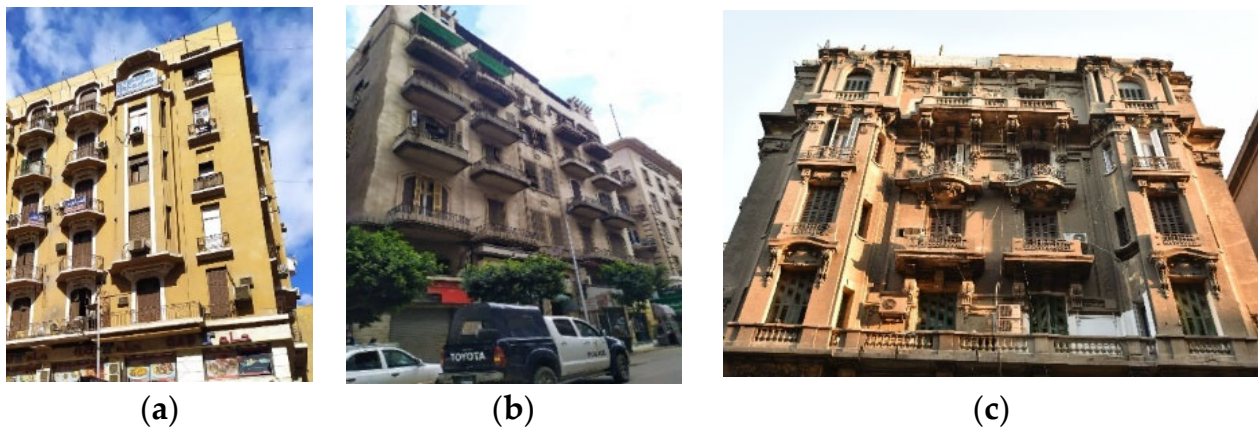


Figure 3. (a) Reference building 7; (b) reference building 8; (c) reference building 9.

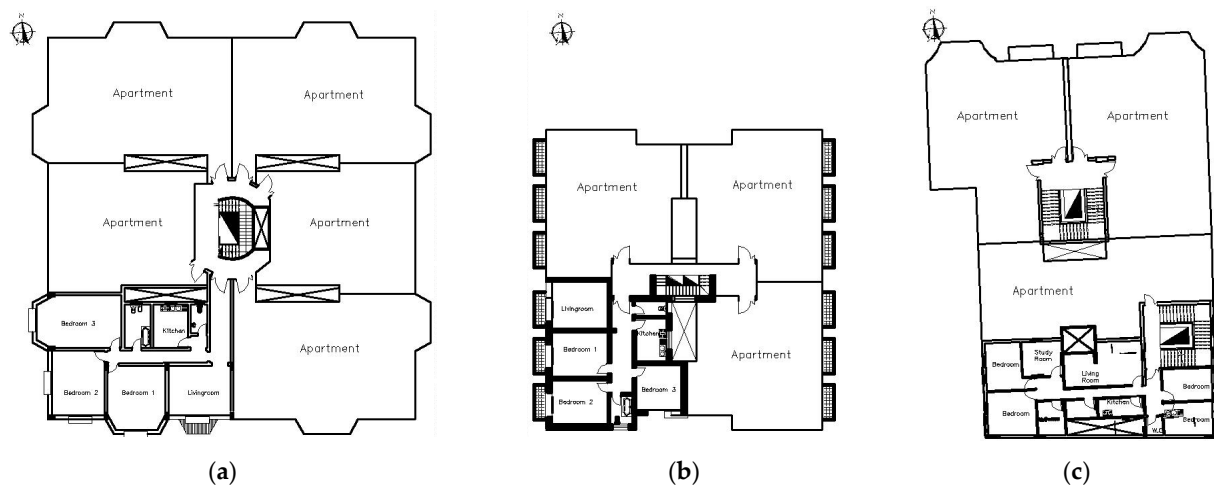


Figure 4. Typical plans of the selected apartments: (a) reference building 7; (b) reference building 8; (c) reference building 9 (based on the first author's Ph.D. research).

2.1.3. Climate Characteristics of the Case Study Area

Location and weather

Cairo is located at latitude 30.1167 degrees north and longitude 31.383 degrees east [12]. The monthly average temperature for July (summer) is between 37 °C (highest degree) and 26 °C (lowest degree), while the monthly average in January (winter) is between 19 °C (highest degree) and 10 °C (lowest degree) [37–39]. Additionally, from 2016 to 2020 in Cairo, the average heating degree days (HDD) with a base temperature of 18.3 °C was 390 days [12], while the average cooling degree days (CDD) during the same period with a base temperature of 10 °C was 4943 days [40–42].

Irradiation data

The annual total radiation was extracted from the Typical Meteorological Year (TMY) weather file of Cairo [12,43]. As a result, we found that the global solar radiation in Cairo reaches up to 2409 kWh/m² annually, with approximately 3300 h of full sunshine. Moreover, the daily solar radiation reaches up to 7.5 in summer and 5.9 kWh/m² in winter [44,45].

2.2. Field Surveys and Interviews

2.2.1. Measurements and Weather Data

The indoor air temperature and relative humidity were monitored in the selected buildings in the winter season of 2021. The selection of date and duration of the field measurements was left up to the residents due to the sanitary measures of COVID-19 restraints. Based on field surveys, measurements were carried out inside living rooms for calibration purposes, because the living rooms were the most occupied spaces in apartments during the day and a large part of the night. The measurements were monitored using a HOBO U12-012 data logger. The hourly measurements were taken in winter for a week. This method was used in some studies such as Ibrahim et al. (2021), Mahar et al. (2019), and Semahi et al. (2019) [12,25,46,47].

2.2.2. Housing and Household Characteristics

Field observations and 230 semi-structured interviews with the residents of the study area (Khedival Cairo) were conducted in summer of 2019 and in winter of 2021. The prepared questions covered the following points: data on the household characteristics, energy consumption, clothing, activity, number of electric appliances and schedules. It should be noted that the purpose behind conducting interviews with many building residents is to ensure that the obtained data represent common housing and household characteristics across building stock in the study area. Moreover, this paper is a part of a Ph.D. research project, and the conducted interviews covered various aspects. In this paper, we selected the most relevant data from the interviews and excluded the rest, included in other work packages of Ph.D. research. Presently, the gathered data, e.g., drawings, details of building materials, and occupancy schedules, were used for building simulation and modeling. In addition, the obtained data were analyzed in depth to understand residents' energy use behavior and calculate the monthly energy consumption of the study area, more specifically of the reference buildings. Additionally, the estimation of average installation power density of the plug loads, lighting and domestic hot water (DHW) were calculated based on the work of Attia et al. (2012, 2015, and 2017) [20,48,49].

2.3. Boundary Conditions

As the main aim of this study is to improve building performance and energy use in heritage residential building stock in the hot, dry climate, defining relevant parameters (variables or constants) is important for simplifying results and encouraging more straightforward ways of interpretation for the readers of this study. Therefore, we assumed that solar heat gains and thermal conductivity are variables. Additionally, we assumed that the internal heat gains, airtightness, and window-to-wall ratio (WWR) are constant values. Due to the lack of measurements of mean radiant temperature (T_{mrt}) in the study area, we assumed that the dry-bulb air temperature is equal to mean radiant temperature (T_{mrt}) and operative temperature (OT), especially where the air velocity is low. Therefore, calibration calculations were carried out considering measured air temperature. Moreover, we addressed only the current orientation of the selected buildings. Furthermore, in this present work, we mainly focused on electricity use as the primary source of cooling, ventilation, heating system, lighting, and plug loads. Moreover, the plug loads of ventilation appliances (ceiling and portable fans) were assumed to be constant.

2.4. Simulation and Calibration

In this work, we selected DesignBuilder software, which is a building energy modeling software package, used to control internal building conditions and provide dynamic analysis of energy consumption [12]. Very recent studies carried out in residential buildings in hot arid climates confirmed the credibility of DesignBuilder for estimating indoor air temperature and energy use [12,25]. Another study carried out by Mahar (2019) proved the credibility of DesignBuilder in Pakistan [46]. Therefore, virtual models were created by using DesignBuilder, based on the actual geometry, construction, and material speci-

fications of the base case buildings (see Appendix A, Tables A1 and A2). Table 1 shows the input data used for building simulation and modeling. The measurement of indoor climate is considered a suitable method for the manual calibration of the virtual model. The temperature data used here are based on hourly data to provide more data points and precision. In this study, the hourly temperature data of one week were used for calibration, and measured in the living rooms of the base case buildings.

Table 1. Input parameters of the base cases (simulation models).

Model Input Measures		Parameters *		
		Reference Building 7	Reference Building 8	Reference Building 9
Envelope	Air tightness (ac/h) at 50 PA **	24.5	21.7	17.9
	WWR (window to wall ratio) (%)	25 N, 21 W, 21 E, 25 S	22 N, 20 W, 20 E, 22 S	18.2 N, 21 W, 21 E
	Window U value ($W/m^2 \cdot K$) single clear 3 mm	5.73	5.73	5.73
	SHGC (solar heat gain coefficient)	0.81	0.81	0.81
	LT (light transmission)	0.898	0.898	0.898
	SC (shading coefficient)	0.99	0.99	0.99
	Roof solar reflectance	0.3	0.4	0.3
Occupancy	Density (people/ m^2)	0.15	0.15	0.04
	Schedules	See Appendix A (Figures A1 and A2)		
Internal load intensities and schedules				
Lighting ***	Installation power density (KW/m^2) living rooms	10	10	0.17
	Installation power density (KW/m^2) bedrooms	6	6	0.13
	Installation power density (KW/m^2) other	2	2	0.9
	Schedules	See Appendix A (Figures A3 and A4)		
	Types	Mix of incandescent and halogen lamps	Mix of incandescent and halogen lamps	Compact fluorescent lamp CFL
Plug loads	Average installation power density (W/m^2) ****	13–15	13–15	13–15
DHW	Period 1 (October–April) ($L/m^2/day$)	0.35	0.35	0.35
	Period 2 (May–September) ($L/m^2/day$)	0.05	0.05	0.05
	Schedules	See Appendix A (Figure A5)		
Ventilation and air conditioning	Temperature setpoint ($^{\circ}C$)	Heating 20, Cooling 22	Heating 20, Cooling 22	Heating 21, Cooling 23
	Coefficient of performance (COP) of air-conditioned units	0.85	0.85	2
	Types of air-conditioned units	Split and window units		
Internal heat gains				
	From lighting (W/m^2)	19		
	From appliances (W/m^2)	12		

Table 1. Cont.

Model Input Measures		Parameters *		
		Reference Building 7	Reference Building 8	Reference Building 9
Activity (metabolic rate)	Metabolism level		1.2	
Clothing	Summer		0.5	
	Winter		1.0	

* Most of the model input values are cross-checked with the work of Attia (2012, 2015, and 2017). ** Airtightness values were calculated based on air change (with a pressure difference between inside and outside of 50 Pa), a method mentioned in the Egyptian code for energy efficiency improvement in buildings [34], inspired by the work of Ibrahim (2021) [12]. *** The lighting profiles are based on the work of Attia et al. (2017) [49]. **** The estimation of average installation power density of the plug loads and DHW were calculated based on the work of Attia et al. (2012 and 2017) [20,49].

For validation of the virtual models, we used ASHRAE Standard 14 and applied the normalized mean bias error (hereinafter, NMBE) and the coefficient of variation of the root mean squared error (hereinafter, CV RMSE) equations; see Equations (1) and (2).

$$NMBE = \frac{\sum_{i=1}^{Np} \cdot (Mi - Si)}{\sum_{i=1}^{Np} \cdot Mi} (\%) \quad (1)$$

$$CV \text{ RMSE} = \frac{1}{M} \sqrt{\frac{\sum_{i=1}^{Np} \cdot (Mi - Si)^2}{Np}} (\%) \quad (2)$$

where Mi and Si are the measured and simulated data at a time interval, and Np and I are the total number of data values used for the calculation.

For further verification, a linear regression analysis was performed to assess the accuracy and correlation between real measurements and simulated ones. This method is used in some studies such as Ibrahim et al. (2021), Mahar et al. (2019), and Semahi et al. (2019) [12,25,46,47].

RETScreen[®] is another software used in a particular part in this work, which is building integrated solar thermal (BIST) [45]. This software estimates some special factors that are not available in DesignBuilder software, such as solar fraction, as elaborated later in Section 2.6.2. To ensure the accuracy of calculations, RETScreen provides an automatic operation with a wide range of equations, e.g., NMBE and linear regression. Presently, we selected a linear regression equation and we ran automatic calibration between two data sets, i.e., real monthly bill gas consumption and heating degree days (HDD). Accordingly, the correlation coefficient (R^2) showed a strong correlation between the two sets of data.

2.5. Applicability of Retrofitting Strategies vs. Heritage Conservation Restraints

To precisely determine the possible retrofitting interventions for the selected buildings in line with the heritage-value perspective, we relied on a checklist of sustainable retrofitting scenarios that we developed in our previous publications [24,25]. This checklist is a matrix of possible retrofitting scenarios in the study area (downtown Cairo), based on three dimensions: heritage value locations, types, and heritage building grades. Therefore, heritage buildings in the study area are classified into three categories, (A), (B), and (C) depending on the importance of the associated heritage values. Our previous study results reveal that all three heritage grades, "A", "B", and "C", are committed to preserving heritage values on an urban district level such as streetscape underground, vistas, etc. Heritage values on urban districts should not be affected by retrofitting scenarios in terms of visual appearance or aesthetic proportions, used materials, and layout. External components or elements include balconies, doors, porches, shopfronts, walls, external wall finishes, external windows, window features, and parapets. However, roofs and roof finishes are excluded, as they can be retrofitted with unlimited interventions without

changing their appearance if they are visible. For example, solar energy (PV and ST) and roof plants are allowed.

2.6. Energy Retrofitting Strategies Analysis

To improve building performance and energy use of the reference buildings, a sensitivity analysis is necessary to test proposed retrofitting intervention scenarios. The proposed interventions are divided into four strategies, as shown in the following subsections:

2.6.1. Passive Retrofitting Strategies

A package of passive retrofitting scenarios was proposed and applied to the base case of the selected buildings. The proposed scenarios are based on hybrid strategies of mixed-mode ventilation, solar and thermal control. The passive retrofitting package includes nocturnal passive cooling, adding white acrylic paint with thickness 0.02 m for the roof, EPS with thickness 0.1 m for walls, and XPS with thickness 0.1 m for the roof. The selection of this passive retrofitting package is based on our most recent study carried out in one of the selected buildings [12]. We addressed and evaluated different passive retrofitting strategies to define the most optimum energy retrofitting scenarios. Accordingly, the selected retrofitting package was evaluated in terms of three performance targets: indoor thermal comfort, the potential energy savings, and compatibility with the conservation of heritage significance. It should be noted that the selected retrofitting package significantly enhanced indoor thermal comfort, i.e., achieves annual comfort hours of up to 66%. Furthermore, this package was highly compatible with the Egyptian Energy Code requirements and cultural values of the building heritage grade. A list of the selected passive retrofitting scenarios can be found in Table 2.

Table 2. A list of passive retrofitting scenarios.

Scenarios	Location	Selected Materials	Thickness (m)	Conductivity (w/m-K)	Specific Heat Capacity (J/kg · k)	Density (kg/m ³)
Package of passive scenarios	Roof	White acrylic paint *	0.02	0.20	1500	1050
	External walls, internal insulations	EPS (expanded polystyrene) **	0.1	0.035	1400	25
	Roof	XPS (extruded polystyrene) **	0.1	0.034	1400	35

* These properties are based on the default materials in the DesignBuilder software (6.1.8.021). ** These properties of materials are extracted from the Egyptian guideline for specifications of building construction materials.

2.6.2. Active Retrofitting Strategies (Non-Energy Generating)

Active retrofitting, non-energy-generating strategies are defined as solutions of mechanical and technological nature that take into consideration, for example, the degree of efficiency of the used appliances and equipment [50].

Replacement of Lighting

Based on the field surveys, we found that most apartments of the selected reference buildings have very low-quality lamps, e.g., incandescent lamps, which affect the indoor climate and energy use. Moreover, a study carried out in Cairo by Attia et al. (2017) tracked lighting energy efficiency in residential buildings over the last 20 years [49]. The study emphasized that replacing incandescent lamps with LED bulbs has great potential for reducing energy consumption. In addition, the Egyptian Ministry of Electricity supplies the domestic market with 10 million LED bulbs to support replacing the conventional lamps with high-quality ones [49]. Accordingly, in this present work, the conventional lighting used in the base case of the reference buildings was replaced with LED lamps.

Replacement of Air Conditioning units

Using effective HVAC systems such as variable refrigerant flow (VRF) is one of the possible solutions to achieve nearly-zero energy buildings [51,52]. Variable refrigerant flow (VRF) HVAC systems have many advantages, making them among the best HVAC systems for heritage buildings [51]. For example, the VRF HVAC systems are associated with light weight, quiet operation, and high efficiency in terms of meeting the loads required for each occupied zone and decreasing power consumption [29,51,52]. Energy savings of up to 55% are predicted when compared to split units [53]. In addition to that, the indoor units of VRF are a perfect visual fit with the building interior, and the outdoor units (compressors) have minimum impact on the building exterior as they can easily be concealed on the building roofs. Furthermore, these systems can help to achieve nearly-zero energy buildings [52]. Therefore, in this study, a VRF cooling system was applied to the base case of the reference buildings. VRF systems may be air- or water-cooled, but our modeling focused on the air-cooled ones. Most of the parameters modeled in this study were extracted from VRF manufacturing guidelines and cross-checked with Afify (2008), Aynur et al. (2009), Kim et al. (2017), Kani-Sanchez et al. (2017), and Torregrosa-Jaime et al. (2018) [52,54–57].

2.6.3. Active Retrofitting Strategies (Energy Generating)

According to Section 2.5, integrating renewable energy sources (RES) in heritage buildings has been very limited due to heritage conservation restrictions. Consequently, only solar energy applications are compatible with cultural value aspects of urban landscape and buildings, including integrating (PV) and (ST). These applications allow good integration with heritage buildings in the Egyptian context. Therefore, these applications were applied to the base cases.

Building Integrated Photovoltaic (BIPV)

In this present work, the application of PV can greatly support the transition towards nearly zero energy heritage buildings [58]. Recently, the PV market has offered a wide range of PV products and brands that can be perfectly integrated in heritage/historic buildings. The selection of a specific PV product depends on various aspects: aesthetic, functional, and technological [58]. Therefore, the application of PV relies on six steps, and this method is used in some studies such as Quintana et al. (2021) [59]. The six steps are explained in detail as follows:

1. Location of PV System

Based on the above subsection, the outdoor roofs of the base cases are the only possible locations that can add PV. Table 3 shows the suggested location and total potential area available for PV application in the base cases.

Table 3. Location and total potential area available for PV application.

Surfaces	Building 7	Building 8	Building 9
Roof area (m ²)	891.85	370.77	773.5

2. Selection of orientation and tilt angle

The orientation of the PV system is an essential factor to ensure that the PV's energy production is maximized. The energy production is influenced by shading on an array of PV caused by other surfaces such as nearby buildings [59,60]. Quintana et al. (2021) recommended that the optimal orientation for PV is to face southwards in the northern hemisphere. In this orientation, the PV receives direct light throughout the day [59]. Additionally, the tilt angle (β) that PV must be set at is considered another important factor for maximizing annual energy production. In most countries in the northern hemisphere, it was found that the best tilt angle (β) to set the PV is when it equals the geographical

latitude (\emptyset) [61,62]. In a previous study carried out by Darhmaoui (2013), the optimal tilt angles to set the PV in the northern part of Egypt are 30.1° and 31.3° [63]. Therefore, in this work, the proposed tilt angle of PV is (30.1°), which equals the geographical latitude (\emptyset) of Cairo at the same time.

3. Selection of PV module

The selection of the PV module is based on module efficiency. Monocrystalline solar panels are more efficient, compared to polycrystalline ones [58,64]. Additionally, monocrystalline panels have a uniform appearance which indicates the purity of silicon crystals. Therefore, PV monocrystalline module panels were selected for this study. The PV module properties can be found in Table 4.

Table 4. Properties of the modeled PV.

Item	Specification	
Component materials		
Cells per module	72	
Cell type	Monocrystalline	
Cell dimensions of the active area	(1700 mm \times 997 mm)	1.69 m ²
Cell dimensions of total area	(1755 mm \times 1038 mm)	1.82 m ²
Weight	19.5 kg	
Performance under standard test conditions		
Maximum power	P _{max}	350 W _p
Open circuit voltage	V _{oc}	44.2 V
Maximum power point voltage	V _{mpp}	37.6 V
Short circuit current	I _{sc}	3.02 A
Maximum power point current	I _{mpp}	2.75 A
Module efficiency	m	19.3%
Thermal characteristics		
Temperature coefficient of short circuit (A/K) *	0.0015402	
Temperature coefficient of open circuit voltage (VK) **	0.13702	

* Temperature coefficient of short circuit = $(TCI 2 \times 0.51)/100 = (30.2 \times 0.51)/100 = 0.0015402$. ** Temperature coefficient of open circuit voltage = open circuit voltage * TC voc, $(44.2 \times -0.31)/100 = 0.13702$. These values were calculated based on specifications of manufactured products available in the international market [65].

4. Selection of PV system size/layout

The number of PV panels and system size were proposed based on the production ratio of PV panel and PV panel wattage sizes (the PV production estimate per module). The production ratio was calculated based on the average electricity consumption in kWh of the apartment per year and the geographic location data of the selected buildings. Table 5 shows the detailed modeled data of PV in each building. It would be possible to maximize the output with extra rows and columns, but that would need in-depth financial and structural feasibility studies [59].

Table 5. PV-required data in terms of module area, number, and total installed capacity.

	Module Area (m ²)	Total Number of Rows	Number of Modules in Rows	Total Number of Modules	Total Installed Capacity (kW)	Total Modules Area (m ²)
Building 7	1.82	4	6	24	8	44
Building 8	1.82	3	5	15	5	27
Building 9	1.82	3	4	12	4	22

5. Inverter selection

This step includes using selected inverters to model conversion from direct current (DC) to alternating current (AC), also known as a power optimizer. The PV panels were connected in parallel with DC junction boxes [59]. Table 6 shows the specifications and controlling parameters of the proposed inverters on Maximum Power Point Tracking (MPPT). The amount of received solar radiation changes overnight, according to the weather conditions that the MPPT used to increase the efficiency output of the PV modules [66,67]. The MPPT controller is a technique used to effectively trace and extract the maximum output values of PV modules and transfer them to the load [66,67], bearing in mind that the specifications of MPPT are provided within various types of inverters in the international market, as shown in Table 6.

Table 6. Parameters of the modeled inverters.

Inverter Parameters	Type
For PV power (kW)	4.0–8.0
Maximum usable input current (MPPT 1/MPPT 2) (A)	18/18
Total max. DC current (A)	36
Max. array short circuit current (1.25 I_{max}) (MPPT 1/MPPT 2) (A)	22.5/22.5
Operating voltage range (V)	80–600
Maximum power point voltage V_{mpp} (V)	600
Short circuit current I_{sc} (A)	22.5
Maximum power point current I_{mpp} (A)	18
Maximum output power (kW)	5
MPP voltage range	240–480
Number of MPPT (V)	2
Maximum efficiency (%)	96.9

All parameters of modeled inverter are extracted from inverter specifications of manufactured products available in the international market [68].

6. Energy storage system selection

Due to variation in power generation by PV, especially during deficit periods, such as between nocturnal and diurnal periods or between summer and winter seasons, the reference buildings must be supported with backup energy [69]. There are different systems to onsite energy storage for later use, such as battery energy storage systems, supercapacitor energy storage systems, and hybrid energy systems [70]. In addition, in the event that the energy storage systems are fully charged, excess electricity will be exported to the grid. Regarding the battery energy storage system, Horan (2021) recommended important factors such as battery type, size, recharging cycles, and lifespan [69]. Several studies and tools have been presented to give an estimation of the best selection of battery size used in residential buildings [71–76]. Supercapacitor energy storage systems reduce stress on the battery energy storage systems during deficit periods [77]. We selected the hybrid energy system, which consists of a battery energy storage system and supercapacitor energy storage system, inspired by a study conducted in similar climate conditions in the United Arab Emirates (UAE) by Salameh et al. (2021). It presented a new integrated hybrid energy system based on battery and supercapacitor energy storage systems [70]. The results (simulation-based) of this work revealed that using a hybrid energy storage system in such a climate is the most effective storage method in terms of the levelized cost of energy and greenhouse gas (GHG) [70]. It is worth noting that in-depth technical analysis of energy storage systems, which requires separate study, is not in our research scope and is far from the study objectives.

Building Integrated Solar Thermal (BIST)

In this present work, the solar thermal (ST) is the second application of RES that is compatible with the selected buildings. The application of ST is linked to the potential saving of primary energy needed for heating space and/or DHW [78,79]. In this study, a typical configuration of the domestic solar water heater SWH system was used. It should be noted that the DHW used in the selected buildings is natural gas-fueled heaters. This system is called an ‘open loop’ passive solar water heater, which is a direct system of circulation to provide hot water to users. Since the climate of Cairo is dry and hot, there is no need to add a heat exchanger with an antifreeze. Moreover, the required data in terms of location selection, orientation, and tilt angle of ST systems were the same as the PV system. As a result, the solar water heater (SWHs) was applied to the roofs of the base cases, including solar collectors, storage tanks, and auxiliary parts, mounted in the south direction with a (30.1°) tilt angle. Additionally, the solar-tracking mode was assumed to be fixed, and miscellaneous losses of the collector were 5%. The fuel type used was natural gas, which is the source of power used for DHW and cooking in most Egyptian residential buildings.

In this subsection, the simulation work was carried out by using RETScreen software [45]. Based on field surveys, the average number of family members was 4.5, which means that an average family consists of 4–5 individuals and the occupancy rate was 80%. Therefore, we assumed that the daily needed hot water use was 0.25 m³, i.e., 250 L per apartment consisting of 5 individuals, operating seven days per week. Accordingly, we assumed the storage capacity of the collector to be 0.07 m³ per area, i.e., 70 L/m², and the total storage capacity to be 0.3 m³, i.e., 300 L. The required load temperature was 55 °C. These assumptions were based on calculations of the total area of each apartment, the number of occupants, average hot water demand of L/m²/day, and solar radiation (kWh/m²/day), inspired by Frattolillo et al. (2020), Lima et al. (2006), and Çomaklı et al. (2012) [78,80–83]. The RETScreen software requires weather data, which can be obtained from the RETScreen Online Weather Database [84], and other data related to users, obtained from interviews with residents. The RETScreen software depends on environmental variables needed to estimate solar energy collected per unit collector area for SWHs. These variables used throughout mathematical models were given by Beckman et al. (1991) (see Appendix B (Equations (A1) and (A2)) [85,86]. Moreover, the collected data were used to calculate the solar fraction, which is an essential indicator in providing the percentage of heating water load supplied by the solar water heaters to the total energy required by the load [79,87,88]. The solar fraction can be estimated by the solar water heater (SWHs) using the f-chart method, clarified in detail by Beckman et al. (1991) (See Appendix B (Equations (A3)–(A5)) [85,86]. Three solar collector types were proposed as shown in Table 7. Moreover, the table also shows their available specifications on the market. The simulation results of the RETScreen software were a solar fraction of the three proposed solar collectors, along with different numbers of collectors.

2.6.4. Hybrid Strategy (Combination of Passive and Active)

To achieve “nearly-ZEB case”, a hybrid retrofitting strategy was applied to the base case buildings. This strategy combines the proposed passive scenarios in Section 2.6.1, active non-energy retrofitting scenarios in Section 2.6.2, and the best obtained results of sensitivity analysis from active energy-generating scenarios in Section 2.6.3.

2.7. Multi-Evaluation

The above-mentioned proposed retrofitting strategies were carried out, and the simulation results of the reference buildings were analyzed and evaluated. This evaluation was based on two performance targets: the potential of energy savings, compatibility with conservation of cultural values, and the Egyptian energy code. It was cross-checked with the work of Ibrahim et al. (2021) [12,25], and with the Egyptian energy code [34]. The simulation results are analyzed and graphically presented in Section 3.

Table 7. Proposed different solar collector types. F_r = overall collector heat removal efficiency factor, U_L = overall heat loss coefficient of a collector [80].

No.	Solar Collector Types *	Optical Efficiency (%)	Collector Gross Area (m ²)	Collector Aperture Area (m ²)	F_r ($\tau\alpha$) Coefficient	$F_r U_L$ Coefficient (W/m ²)/°C	Temperature Coefficient for $F_r U_L$ (W/m ²)/°C	Source
1	Unglazed flat-plate collectors	95	4.367	4.367	0.816	0.84	0.03	SRCC 100-2004-012A
2	Glazed flat-plate collectors	82.4	2.31	2.05	0.71	3.95	0	SPF C300
3	Tubular evacuated collectors	76	2.28	2	0.56	15.763	0	DIN 011-7S113R

* Most of these parameters of solar collector types were extracted from RETScreen software and manufacturer specifications of the products from Aquatherm Industries, Soltop Schuppisser, and Shangdong Linuo Paradigma, for type 1, 2, and 3, respectively [89–91], and these specifications were cross-checked with [79,87,92].

3. Results

3.1. Modeling and Validation

To calibrate the simulation models, the NMBE and CV (RMSE) equations were applied as per ASHRAE Standard 14, according to acceptable limits as mentioned in Section 2.4. The measured indoor air temperatures were used to calibrate the simulation models, and data for temperatures measured in living rooms for a week in winter were compared. Figure 5a–c shows a comparison of the measured and simulated indoor temperatures for the observation periods. The models were manually calibrated, and several adjustments were made, including schedules of occupancy and lighting. The values of NMBE and CV (RMSE) (NMBE) for the calibrated models can be found in Table 8. These values do not exceed the recommended limits mentioned in ASHRAE Standard 14. Accordingly, the simulation models were calibrated using hourly data. Linear regression was analyzed to verify the calibration accuracy and the correlation between simulated and measured data. The correlation coefficients (R^2) of 0.971, 0.902, and 0.943 for reference buildings 7, 8, and 9, respectively, show a strong correlation for calibration verification (see Appendix A, Figures A6–A8).

Table 8. Validation summary of the calibration criteria of the simulation model.

	Validation Criteria	
	NMBE (%)	CV(RMSE) (%)
R. Building 7	−0.02	1.02
R. Building 8	0.02	0.93
R. Building 9	0.01	0.5

3.2. Evaluation of the Base Case Status

The simulation results of the base case of the three models can be found in Figure 6. This figure shows the simulated monthly consumption of electricity and natural gas of the base case in the reference buildings. Overall, the electricity consumption of the three models from April to September was higher than all the rest. However, natural gas consumption of the three models at the same time was lower than all the rest. The total electricity consumption of reference buildings 7, 8, and 9 was 84, 66.8, and 46.9 kWh/m²/year, respectively. Additionally, we found that the electricity consumption breakdown of the base case of reference building 7 was 45.4 kWh/m²/year cooling, 12.3 kWh/m²/year heating, 15.4 kWh/m²/year lighting, and 10.8 kWh/m²/year plug loads and other miscellaneous items (lifts, water pumps, etc.), whereas the electricity consumption breakdown of the base

case of reference building 8 was 30 kWh/m²/year cooling, 11.4 kWh/m²/year heating, 15.1 kWh/m²/year lighting, and 10.5 kWh/m²/year plug loads and miscellaneous items. Building 9 was 25.54 kWh/m²/year cooling, 6.1 kWh/m²/year heating, 5.3 kWh/m²/year lighting, and 10.1 kWh/m²/year plug loads and miscellaneous items. Moreover, it was found that the total natural gas consumption per apartment of the base case in reference buildings 7, 8, and 9 was 623.76, 551.39, and 602.31 kWh/ year, respectively.

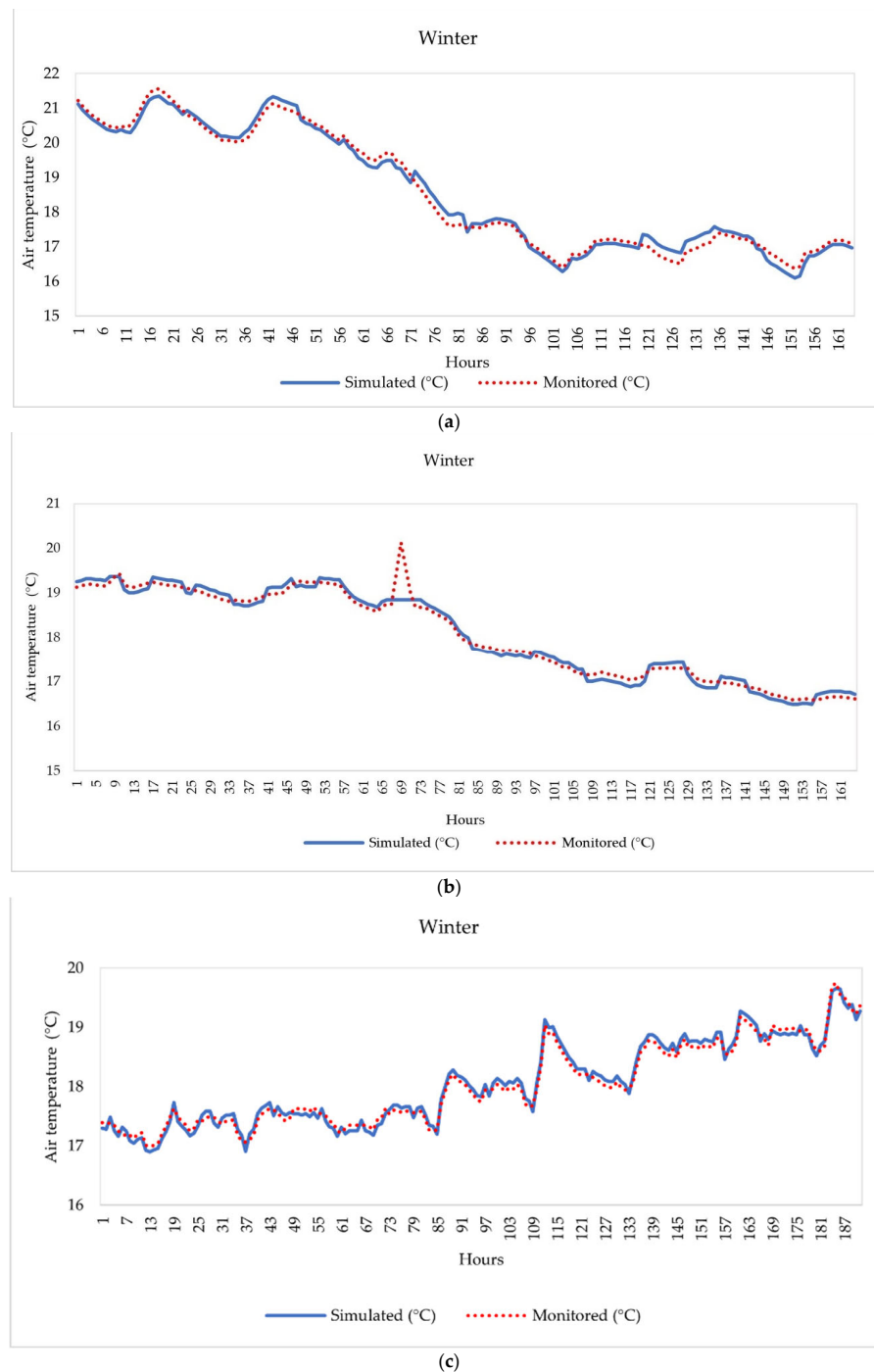


Figure 5. Validation of the calibration based on measured and simulated air temperature in the living room of the selected base case during winter 2021. (a) Reference building 7, (b) reference building 8, (c) reference building 9.

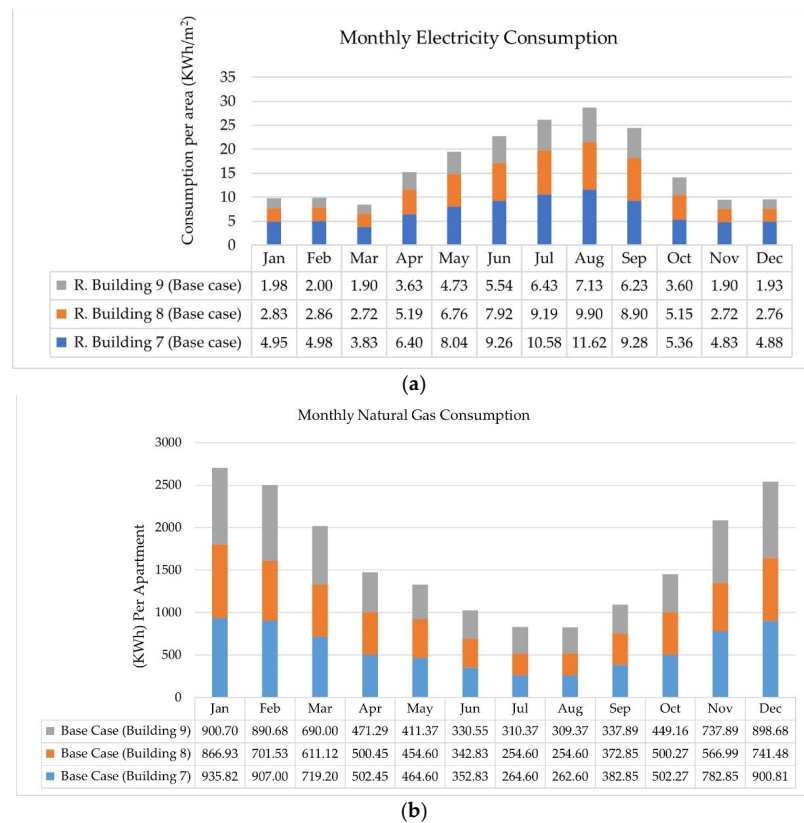


Figure 6. (a) Monthly electricity consumption and (b) monthly natural gas consumption of the base case buildings.

3.3. Effect of Passive Strategies

The proposed package of passive scenarios was applied to the base case buildings, and the simulation results can be found in Figure 7. It shows the simulated monthly electricity consumption of the three models. Overall, it can be noted that this package of passive scenarios greatly improved electricity use throughout the year compared with the base case; see Figures 6a and 7. The application of this package reduced the electricity consumption of the base case in reference building 7 from 84 to 43.5 kWh/m²/year, reference building 8 from 66.9 to 41.3 kWh/m²/year, and reference buildings 9 from 46.9 to 20.5 kWh/m²/year.

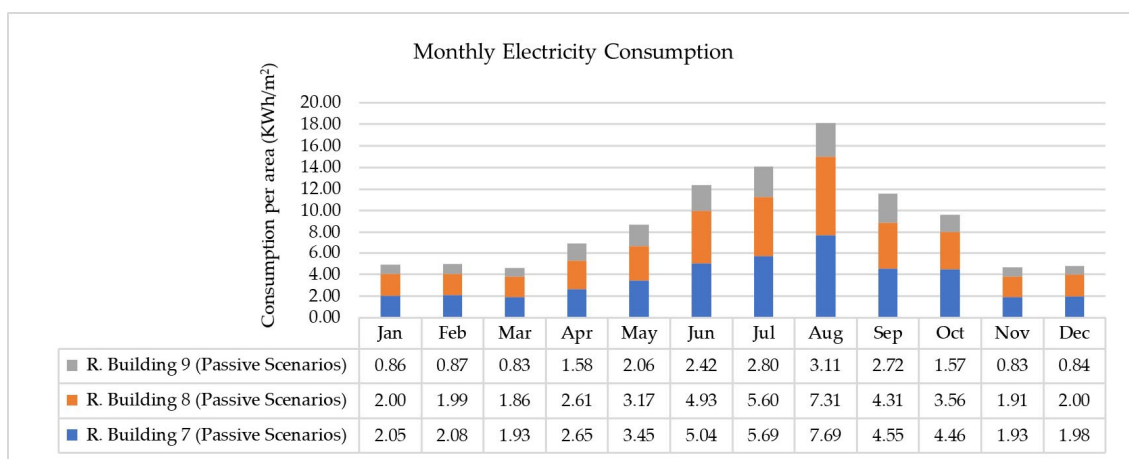
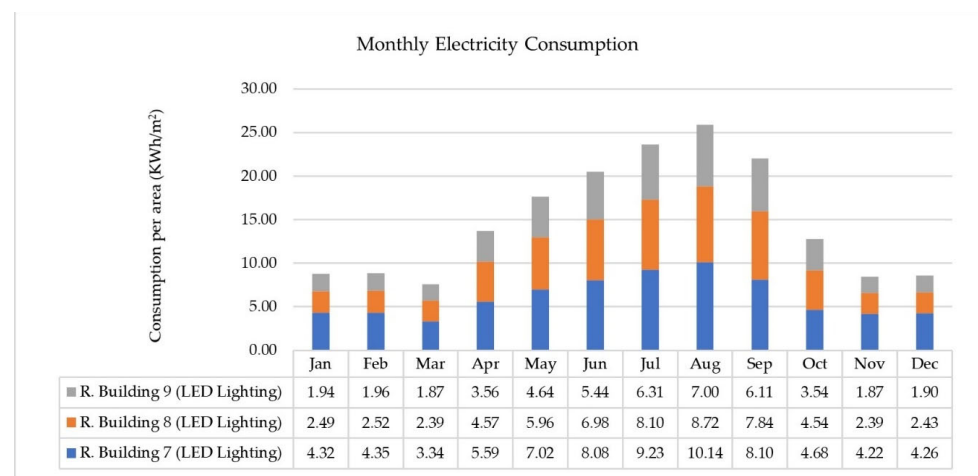


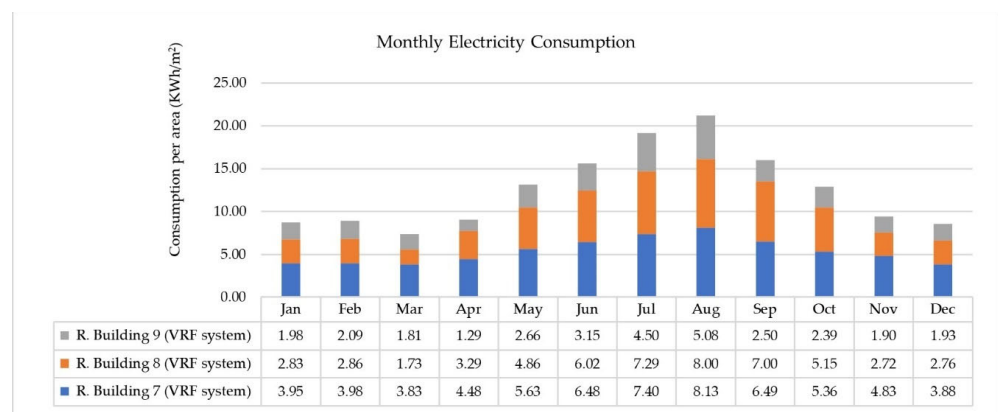
Figure 7. Monthly electricity consumption of the three models after applying a package of passive scenarios.

3.4. Effect of Applying Active Strategies

The proposed active scenarios, LED lighting and VRF HVAC systems were applied to the base case buildings; the simulation results can be found in Figure 8. This figure shows the simulated monthly electricity consumption of the three models. The application of the active scenario, replacing the conventional lighting lamps with LED lighting ones, reduced the electricity consumption of the base case in the reference buildings, as shown in Figure 8a. The electricity consumption of reference buildings 7, 8, and 9 was reduced from 84 to 73.3 kWh/m²/year, from 66.9 to 58.9 kWh/m²/year, and from 46.9 to 46.14 kWh/m²/year, respectively. The application of the active scenario of replacing the split air conditioning units with VRF HVAC systems reduced the electricity consumption of the base case in the reference buildings, as shown in Figure 8b. The total annual electricity consumption of reference buildings 7, 8, and 9 was reduced from 84 to 64.5 kWh/m²/year, from 66.9 to 54.5 kWh/m²/year, and from 46.99 to 31.29 kWh/m²/year, respectively.



(a)



(b)

Figure 8. Monthly electricity consumption of the three models after applying a package of active scenarios. (a) LED lighting, (b) VRF HVAC system.

3.5. Effect of Combination between Passive and Active Strategies

A combination of the proposed passive and active packages was applied to the base-case buildings, and the simulation results can be found in Figure 9, where the simulated monthly electricity consumption of the three models is shown. Overall, the application of these packages greatly improved electricity use throughout the year compared to the base case, as shown in Figure 9. More clarifications about these results are explained in the discussion section. The electricity consumption of reference building 7 was reduced

from 84 to 28.2 kWh/m²/year, as shown in Figure 9a. The electricity consumption of reference building 8 was reduced from 66.9 to 26.8 kWh/m²/year, as shown in Figure 9b. In addition, the electricity consumption of reference building 9 was reduced from 46.9 to 18.5 kWh/m²/year, as shown in Figure 9c.

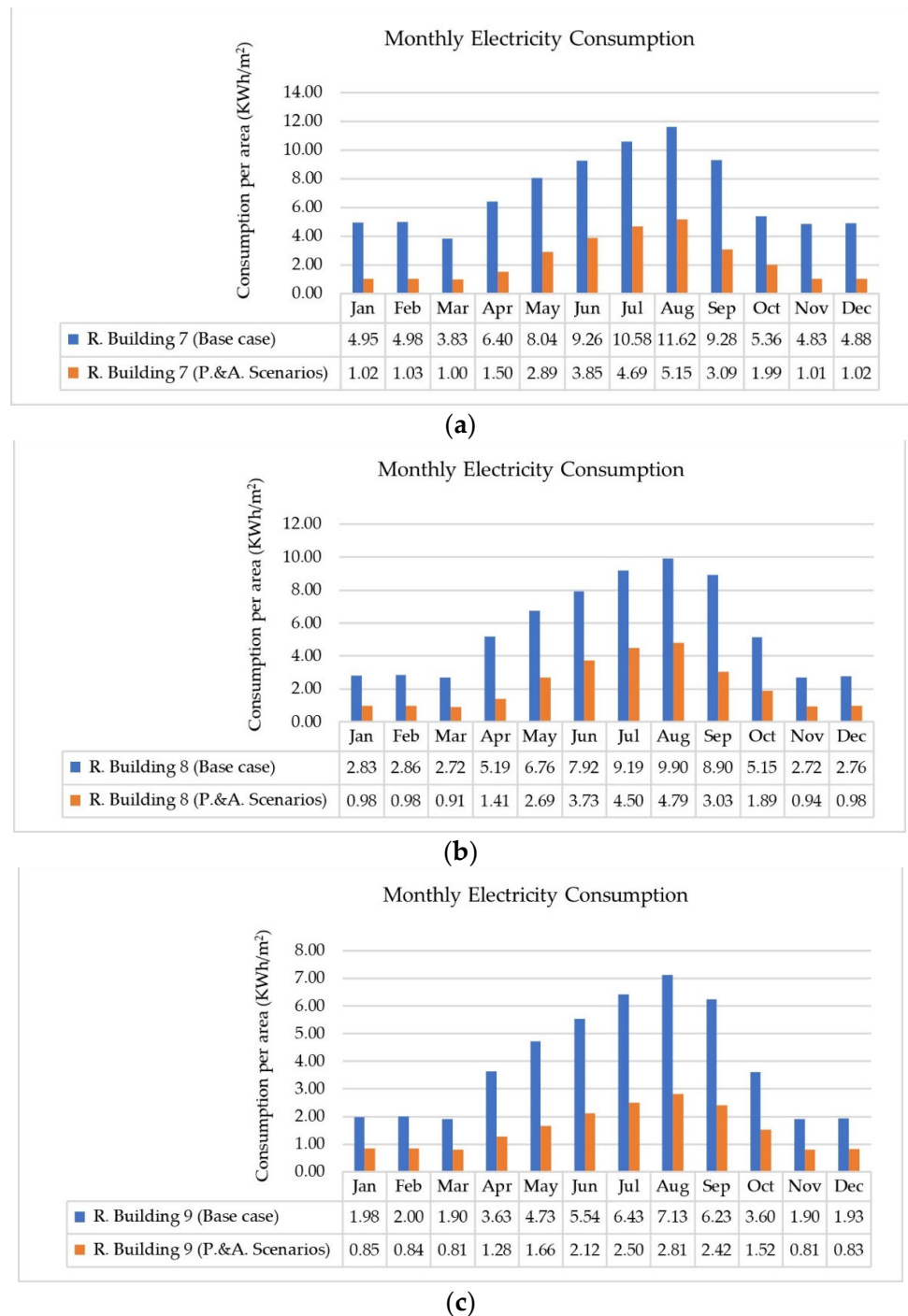


Figure 9. Monthly electricity consumption of the three models after applying combination of passive and active scenarios. (a) Reference building 7, (b) reference building 8, (c) reference building 9.

3.6. Effect of Building Integrated Photovoltaic (BIPV)

The simulation results of integrating solar photovoltaic cells to the base case in the reference buildings can be found in Figure 10 and Table 9. Figure 10 shows both the simulated monthly electricity consumption and generation of the three models. In building

7, it was found that the implementation of PV met electricity demand, generating 120.4% of building electricity needs on an annual basis. However, by analyzing monthly electric output, the consumption during July and August of the base case exceeded the generation, as shown in Figure 10a. Similarly, in building 8, it was found that the implementation of PV met the electricity demand, by generating 125.8% of the building's electricity needs on an annual basis. Moreover, the electricity output was analyzed monthly, and it was found that the electricity consumption of the base case in June, July, and August exceeded the generation, as shown in Figure 10b. Building 9 generated 123.4% of the building's electricity needs on an annual basis. Additionally, by analyzing the electricity output every month, the electricity consumption of the base case in June, July, August, and September exceeded the generation, as shown in Figure 10c.

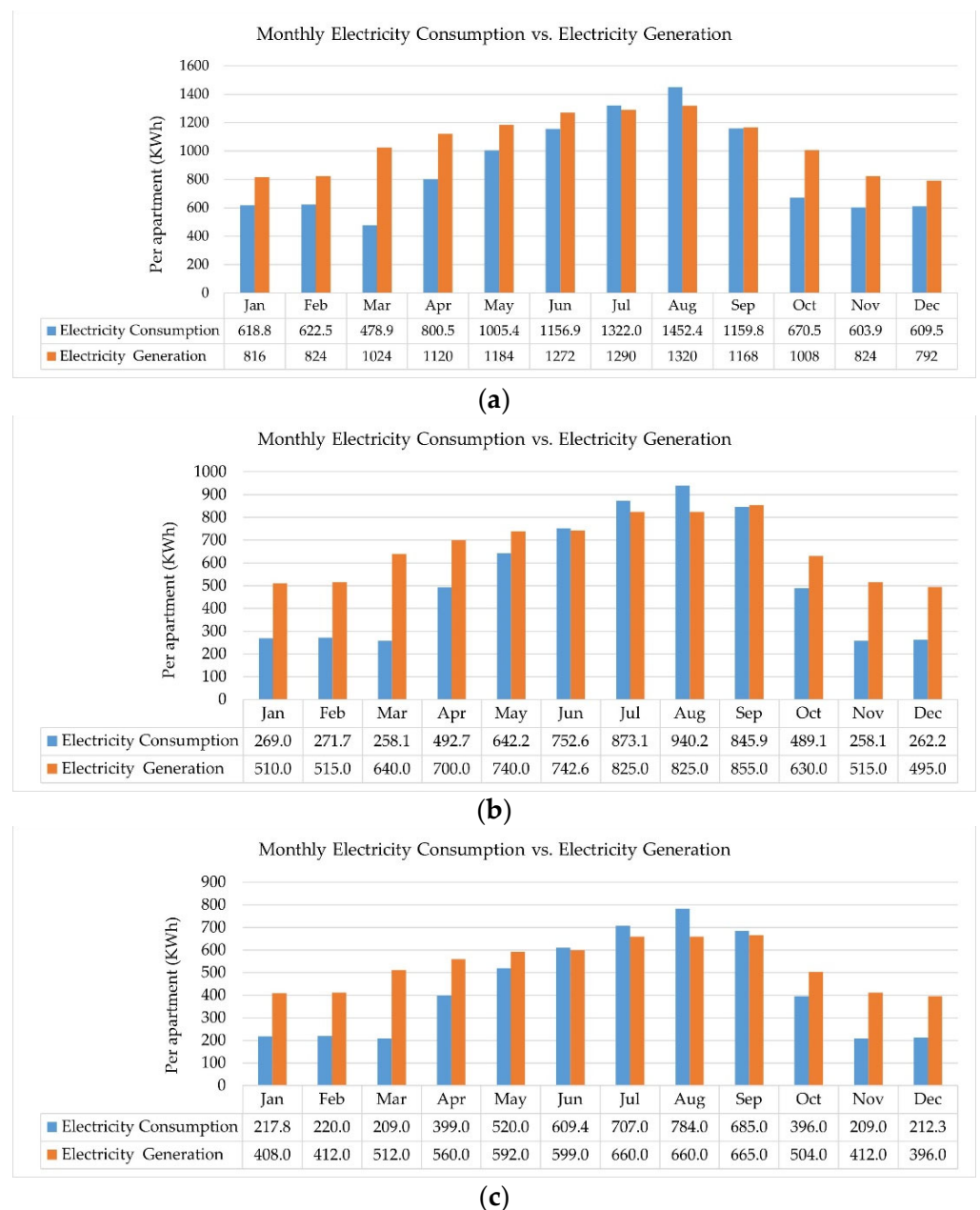


Figure 10. Comparison between monthly electricity consumption of the base case and generation electricity by PV cells. (a) Reference building 7, (b) reference building 8, (c) reference building 9.

Table 9. Summary of annual (KWh per apartment) electricity consumption, generation, self-consumption of generated PV electricity, and electricity coming from utility and going to utility.

	Building 7		Building 8		Building 9	
	Electricity (kWh/year)	Electricity (%)	Electricity (kWh/year)	Electricity (%)	Electricity (kWh/year)	Electricity (%)
Electricity Consumption	10,501.0	100.0	6354.9	100.0	5168.4	100.0
Electricity Generation	12,642.0	120.4	7992.6	125.8	6380.0	123.4
Self-consumption	8187.4	78.0	4822.9	75.9	3882.4	75.1
Power Conversion + Losing	2149.1	20.5	1358.8	21.4	1084.6	21.0
Electricity Coming from Utility	2313.6	22.0	1532.0	24.1	1285.9	24.9
Surplus Electricity Going to Utility	2141.0	20.4	1637.7	25.8	1211.6	23.4

3.7. Effect of Building Integrated Solar Thermal (BIST)

The simulation results of the RETscreen software of the proposed solar collectors applied to the three reference buildings can be found in Figure 11. Figure 11a shows solar fractions for unglazed, glazed, and evacuated solar collectors in the three reference buildings. In the selected buildings, the solar fraction reaches up to 100% if the solar collectors are two unglazed or evacuated ones, while it reaches up to 90% if the solar collectors are two glazed ones. Moreover, the solar fraction is mostly similar (up to 40%) using one unglazed collector. Up to 60%, a solar fraction can be reached if the solar collector is only one glazed collector in the selected buildings or an evacuated collector about building 9, whereas up to 70% can be reached with one evacuated collector in reference buildings 7 and 8. Figure 11b shows the energy (natural gas) saving potential in these buildings. Unglazed solar collectors have greater potential for annual energy saving if two solar collectors are used. On the other hand, unglazed solar collectors have a lower value than glazed and evacuated ones if only one collector is used. Additionally, two evacuated solar collectors might have greater potential for annual energy saving than glazed ones. For one collector, an unglazed solar collector saved 1665.6, 1282.4, and 1429.3 KWh/apartment per year in buildings 7, 8, and 9, respectively, whereas the glazed solar collector saved 2329, 2002, and 2810.9 KWh/apartment per year and the evacuated solar collector saved 2785, 2395.3, and 2995.2 KWh/apartment per year in buildings 7, 8, and 9, respectively.

3.8. Evaluation of the “Nearly-ZEB Case”

The proposed “nearly-ZEB case” impact on energy improvements was analyzed among three reference buildings, as shown in Table 10. The table evaluates each proposed scenario separately in terms of energy improvement and compatibility with local legislation. The proposed nearly-ZEB case includes passive, active, non-energy-generating, and energy-generating scenarios. The case shows annual energy improvements of applying passive and active retrofitting scenarios, excluding the application of PV and SWH, and the application of PV and SWHs was analyzed and evaluated previously in Sections 3.5 and 3.6. As a result, the application of two unglazed solar collectors was selected as the best-obtained scenario of SWHs. Additionally, this case achieved two performance targets: potential energy saving and conservation of cultural values. Furthermore, indoor thermal comfort was another performance target that can be automatically achieved based on passive retrofitting scenarios, as will be explained in the discussion section.

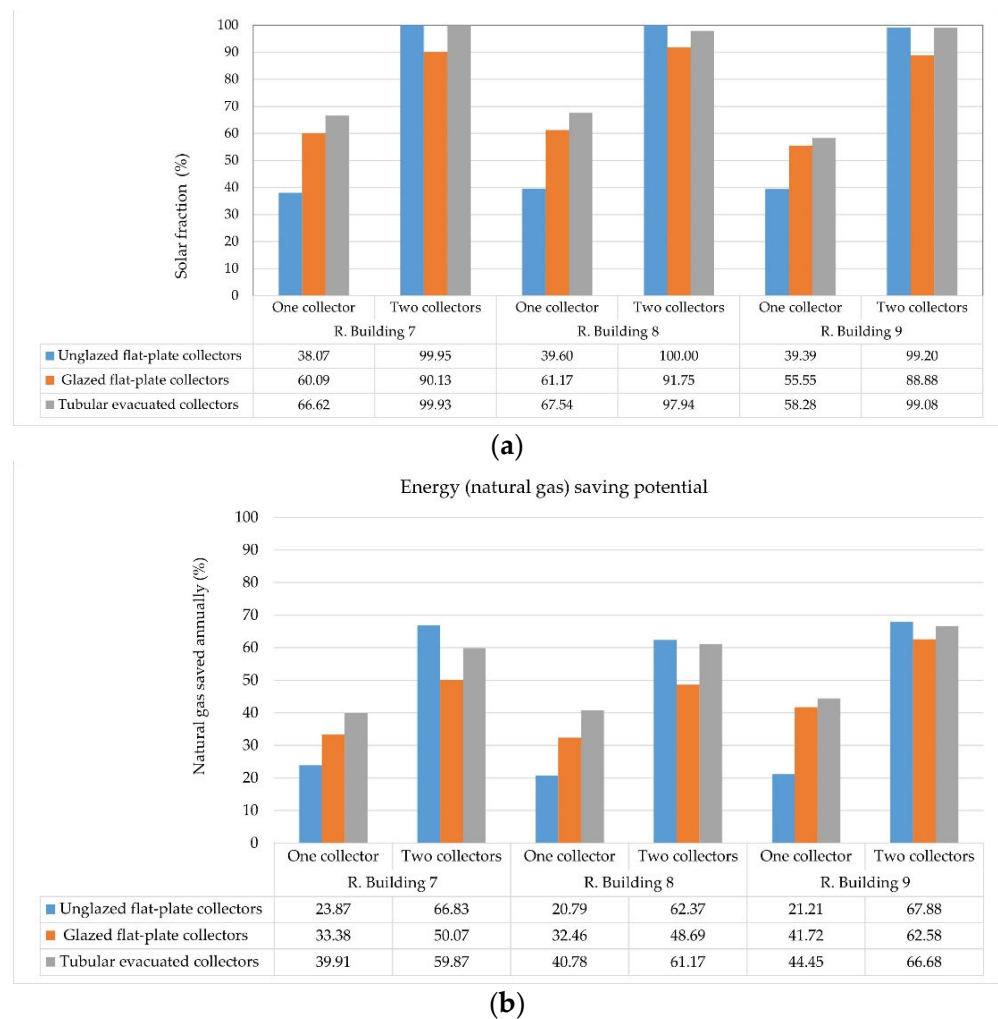


Figure 11. (a) Solar fraction for unglazed, glazed, and evacuated solar collectors in the three buildings, and (b) energy (natural gas) saving potential in the three buildings.

Table 10. Evaluation of the proposed retrofitting strategies.

Strategy	Description	** Energy Improvements (%)			*** Compatibility with Egyptian Energy Code	*** Compatibility with the Limits of the Interventions Allowed in Heritage Grade B		
		Building 7	Building 8	Building 9		Visual	Physical	Spatial
* Passive strategy	A set of passive scenarios (nocturnal cooling, solar and thermal control)	48.2	38.3	56.3	✓+	✓+	✓+	✓+
Active non-energy generating	LED lighting	12.7	11.9	1.8	✓+	✓+	✓+	✓+
	VRF HVAC systems	23.3	18.5	33.4	✓+	✓+	✓+	✓+
Active energy-generating	Application of PV modules	See Figure 10 and Table 9			✓+	✓+	✓+	✓+
	Application of ST collectors	See Figure 11			✓+	✓+	✓+	✓+
Nearly-ZEB case	Combination of passive and active (LED+ VRF) scenarios	66.4	59.9	60.7	✓+	✓+	✓+	✓+
	Application of PV modules	See Table 9			✓+	✓+	✓+	✓+
	Application of two unglazed solar collectors	See Figure 11b			✓+	✓+	✓+	✓+

* This set of passive scenarios raised the annual indoor thermal comfort of the reference building 9 from 31.4% to 65.9% from the total hours, based on the work of Ibrahim et al. (2021) [12]. ** Energy improvements refer to the electricity saving potential of all proposed scenarios except SWHs scenario, which refers to natural gas saving potential. *** This evaluation was based on the work of Ibrahim et al. (2021) [12,24,25]. (✓+) means highly compatible.

4. Discussion

The results of this study are discussed in three sub-sections: main findings and recommendations, strengths and limitations of the study, and study implications and future research.

4.1. Main Findings and Recommendations

The main findings of this study show the applications of the four phases of the proposed retrofitting methodology and the outcome from methodology application.

1. Phase one selects real reference buildings representing the most dominant residential building types in the case study area, Khedivial Cairo. Indoor air temperatures inside the selected buildings were monitored, and three energy models were created, simulated, and manually calibrated.
2. Phase two evaluates the building envelope and energy performance of the three models, as base cases. The detailed evaluation process is as follows:

Base case evaluation

The simulation of the base case models was performed to determine the building energy performance of the heritage residential buildings. Overall, by analyzing the building envelope performance of the selected buildings, we found that these buildings did not provide minimum requirements for the values of energy efficiency for the Cairo climate, which are stated in the Egyptian Energy Code for energy efficiency improvement in buildings, Part 1(ECP 306–2005) [34]. On the one hand, the thermal resistance (R) values of the building envelope (opaque) of the base case reference buildings 7 and 9 were exactly typical. The values of roofs and external walls were 0.18 and 0.53 ($\text{m}^2 \cdot \text{k}/\text{w}$), respectively, whereas the thermal resistance (R) values of roof and external walls of the base case reference building 8 were 0.40 and 1.2 ($\text{m}^2 \cdot \text{k}/\text{w}$), respectively. Both thermal resistance (R) values of roofs and external walls were very low, more specifically in buildings 7 and 9, whereas thermal resistance (R) values of roofs and external walls of building 8 were better than the other two, thanks to the different construction materials (see Appendix A, Table A2). In some external walls, R values met the minimum requirement. Additionally, the airtightness was calculated and assumed to be a constant value, due to the lack of measurements of airtightness in the study area. These calculations were based on the air change method, which is stated in the Egyptian code for energy efficiency improvement in buildings and inspired the work of Ibrahim et al. (2021) [12]. The airtightness values were 24.5, 21.7, and 17.9 air changes per hour (ach/h) of buildings 7, 8 and 9, respectively.

Moreover, by analyzing the monthly energy consumption, we found that a large portion, approximately 50%, of electricity consumption was used for cooling in the three models. This is due to a very low building envelope performance and indoor thermal comfort conditions, which led to higher electricity consumption for cooling. About 22% of electricity usage was for lighting, especially in buildings 7 and 8 that use a mix of incandescent and halogen lamps. However, about 11% of the electricity used for lighting was in building 9, which uses compact fluorescent lamps (CFL). Overall, the annual electricity consumption of building 9 was lower than buildings 7 and 8. Both buildings 7 and 8 are freestanding, while building 9 has one adjacent wall. As a result, the limited exposed surface area of the external walls of building 9 led to reduced heat gains. Similarly, the airtightness of building 9 was lower than buildings 7 and 8 for the same above-mentioned reason.

3. Phase three determines cultural value restrictions of the heritage grade of the selected buildings and proposes appropriate retrofitting scenarios. We found that all selected buildings have the same heritage grade, "Grade B", which is the most dominant in the study area. The proposed retrofitting scenarios followed a retrofitting checklist provided by Ibrahim et al. (2021) [24,25]. In the first step, proposed passive retrofitting scenarios were applied. Secondly, proposed active non-generating and generating scenarios were applied separately. Lastly, a combination of passive and active retrofitting

scenarios was applied and evaluated as “nearly-ZEB case”. The evaluation process is as follows:

Step1: Evaluation of passive retrofitting scenarios

The application of the passive retrofitting package consists of nocturnal passive cooling, cool roofing, and internal insulation for the external walls and roofs. The evaluation of this package includes building envelope and energy consumption. By applying this package, the results show that the building envelope was significantly improved in the three models. This package improved both the thermal resistance (R) values of roofs and external walls of the base case buildings. The thermal resistance (R) values of the roofs of buildings 7 and 9 were improved by 94% and building 8 by 89.9%, compared to the base case. Moreover, the external walls of buildings 7 and 9 were improved by 83.4% and building 8 by 69.4%. As a result, the annual reduction in the total electricity consumption of buildings 7, 8, and 9 were 48.2%, 38.3%, and 56.3%, respectively. Additionally, the annual reduction in the cooling electricity consumption of reference buildings 7, 8, and 9 was 62.6%, 47.1%, and 70.5%, respectively. In addition, up to 100% of the annual reduction in heating electricity consumption of the three reference buildings could be achieved, as heating demand was eliminated because of insulation materials applied to roofs and external walls. This retrofitting package greatly enhances indoor thermal comfort.

Step2: Evaluation of active (non-energy generating) retrofitting scenarios

The analysis and evaluation of the active retrofitting scenarios consist of LED lighting and a VRF cooling system. By applying LED lighting, we found that the annual reduction in the total electricity consumption of buildings 7, 8, and 9 was 12.7%, 11.9%, and 1.8%, respectively. Additionally, the annual reduction in the lighting electricity consumption of reference buildings 7 and 8 was 60.5%, while building 9 was only 7.9% due to the different types of lighting used, as mentioned above. By applying the VRF HVAC system, the annual reduction in the total electricity consumption of buildings 7, 8, and 9 was 23.3%, 18.5%, and 33.4%, respectively. Additionally, the annual reduction in the cooling electricity consumption of reference buildings 7, 8, and 9 was 43%, 41.3%, and 61.5%, respectively.

Step 3: Evaluation of a combination of passive and active retrofitting scenarios

By applying a combination of passive and active non-energy-generating scenarios, maximum energy savings could be achieved relative to the base case. The total electricity savings per year were 66.4%, 59.9%, and 60.7% for buildings 7, 8, and 9, respectively. Moreover, the electricity savings per year for cooling were 70.7%, 58.7%, and 78.3% for buildings 7, 8, and 9, respectively. On the contrary, the electricity savings per year for plug loads and miscellaneous were 18.5%, 19.1%, and 19.9% for building 7, 8, and 9, respectively. Accordingly, the electricity consumption breakdown for building 7 was 13.3 kWh/m²/year cooling, 6.1 kWh/m²/year lighting, and 8.8 kWh/m²/year plug loads and miscellaneous, whereas for building 8, the electricity consumption breakdown was 12.4 kWh/m²/year cooling, 5.9 kWh/m²/year lighting, and 8.5 kWh/m²/year plug loads and miscellaneous. For building 9, the electricity consumption breakdown was 5.5 kWh/m²/year cooling, 4.9 kWh/m²/year lighting, and 8 kWh/m²/year plug loads and miscellaneous. It can be noted that by applying the combination of passive and active scenarios, the annual electricity used per area for heating, lighting, and plug loads in the three buildings was approximately similar except for the electricity used for cooling, where the electricity used for the cooling of buildings 7 and 8 was almost double the one used of building 9. As a result, the total electricity consumption of buildings 7 and 8 was higher than the electricity consumption of building 9. The reasons behind that might be building typology affecting energy consumption, due to buildings 7 and 8 belonging to the same main building typology with different construction material types [24].

Step 4: Evaluation of active (energy-generating) retrofitting scenarios

By integrating solar photovoltaic cells into the reference buildings, the results show that the implementation of PV met the demand for electricity generation of the buildings

on an annual basis. However, by analyzing the monthly electricity output, it was found that the electricity consumption of the base case in summer exceeded the generation. On the other hand, electricity generation in winter exceeded the consumption of the three buildings, where self-consumption was 78%, 75.9%, and 75.1% of buildings 7, 8, and 9, respectively. In addition, the electricity coming from utility (government grid) was 22%, 24%, and 24.9% of buildings 7, 8, and 9, respectively, whereas the surplus electricity going to utility was 20.4%, 25.8%, and 23.4% of buildings 7, 8, and 9, respectively. By integrating solar thermal using SWHs to the reference buildings, the results show that two unglazed solar collectors saved more energy compared to the other two types of collectors. Reference building 8 showed greater energy saving potential than the other buildings for the two unglazed, glazed, and evacuated collectors. Moreover, solar fraction also increased as the number of collectors increased for two evacuated and glazed collectors. Reference building 8 was the best among the selected buildings, while other buildings received 100% solar fraction by using two unglazed collectors. It should be noted that analysis of the natural gas usage is not within the scope of our research, but energy-saving potential for the natural gas was mentioned as an indicator of the effectiveness of using different types of SWHs collectors, as natural gas was mostly used for cooking and domestic hot water in the residential buildings in Egypt.

4. Phase four evaluates all the above-proposed scenarios to define the “nearly-ZEB case” and its compatibility with local legislation, and to apply it to 133 heritage residential buildings in the study area. The proposed nearly-ZEB case includes passive, active, non-energy-generating, and energy-generating scenarios. This case has the most effective retrofitting solutions in terms of three performance targets: indoor thermal comfort, achieving nearly-zero energy use, and compatibility with cultural values.

Finally, to summarize the benefits of the proposed methodology, we list a set of recommendations below:

- A. Selecting reference buildings that represent the most dominant building typologies on the urban level of a study area is considered a tool of flexibility and strength that could provide preliminary advice on energy performance and sustainable scenarios for retrofitting.
- B. Operative temperature (OT) should be considered in thermal comfort and energy use calculations. As mentioned previously in Section 2.3, air temperature measurements were used to carry out the manual calibration. It should be noted that there was a peak point that occurred in the measured air temperature in reference building 9, because the number of occupants unusually increased for two hours during nighttime; see Figure 5b. However, this unexpected change had no noteworthy effect on overall calculations of calibration and energy.
- C. Application of a set of passive energy-efficient scenarios provides maximum primary energy saving, taking into consideration that different building typologies with similar energy retrofitting interventions have a different impact on energy savings under the same climate conditions. It should be noted that both building size and location could affect the energy retrofitting strategies applied. However, in our present work, they had no noteworthy effect, because all reference buildings have approximately similar sizes and locations.
- D. Replacing conventional lighting lamps with LED lighting would achieve optimal lighting energy efficiency, especially in developing countries with hot climates.
- E. Replacing air conditioning units (AC) with VRF HVAC systems in apartment buildings would be an effective solution to achieve nearly-zero energy buildings. However, energy savings with this system could occur at moderate temperature conditions (not exceeding 35 °C), whereas at high temperature conditions, VRF could consume more energy compared to the other HVAC systems [93]. Moreover, feasibility and financial studies of replacing air conditioning units (AC) with VRF HVAC systems should be considered.

- F. The application of PV in residential building stock should have a dual meter—bidirectional meter—if the installation of a solar energy system is connected to the government grid, to calculate the amount of energy produced by the solar panels and the amount of energy consumed. As a result, the residents' net bills are either positive or negative.
- G. Feasibility studies are required for the integration of PV in residential buildings. That includes a financial study of PV; for example, the initial cost, payback period, and electricity prices from and to the government grids.
- H. In hot climates, to maximize the benefits of PV applications on the urban level, investigations should be conducted in terms of determining the exact electricity demand—monthly and daily peak loads—to effectively define the solar electricity generation needed.
- I. By application of ST using SWHs, the evacuated type of solar collector is considered most efficient if one solar collector is used, but this type is generally more expensive due to the added cost of creating a vacuum [79]. The unglazed type is the cheapest and most efficient if two solar collectors are used. However, it requires a large area to effectively heat the needed amounts of water [79].
- J. In hot climates, unglazed collectors could be an effective option to provide a large amount of water (below 40 °C) for domestic hot water supplies. Glazed flat-plate collectors are the most widely used and can provide heat for basic domestic hot water use (below 60 °C). On the other hand, evacuated tube collectors can deliver heat at high temperatures (above 80 °C) and is higher in efficiency compared to flat-plate collectors [79,87,88]. Similarly to the application of PV, the application of SHWs requires feasibility and financial studies.
- K. The proposed “nearly-ZEB case” of the three reference buildings could be used as benchmark energy models in heritage residential building stock of Khedivial Cairo. Furthermore, the proposed methodology would cover the maximum energy needed by using the energy generated by solar energy, and export surplus energy, if applicable, to energy grids. More importantly, this methodology would improve the indoor thermal comfort and be highly compatible with the Egyptian Energy Code requirements and cultural values of the different building heritage grades.

4.2. Strengths and Limitations of the Study

The strengths of this study lie in the combination of real monitoring datasets with an advanced simulation of building performance and manual calibration. Moreover, this study identifies the most effective energy conservation measures that combine a set of passive and active strategies to improve both energy use and indoor thermal comfort. Furthermore, this work evaluates the potential of using new technologies on heritage buildings that belong to an important historical vintage era (Khedivial era). Other strength points of this study lie in providing a precise and clear framework of applying (PV) in heritage residential building stock and highlights its potential to achieve the nZEB target in hot climates. Moreover, the paper compares three different solar collector types for SWHs to provide the most effective type to be used in hot climates. This work is distinct from the previous works of Bellia et al. (2015) and Şahin et al. (2015) that assess the risk levels of proposed retrofitting scenarios on cultural values. In contrast, our work determines possible interventions in each heritage significance grade to ensure preserving cultural values. It is also distinct from the work of Güleröglu et al. (2020) that did not include enhancing indoor thermal comfort as a target, despite carrying out their study in a hot climate, and enhancing indoor thermal comfort is considered a basic requirement in such climates. On the other hand, our findings confirm the statement of Lucchi et al. (2020) and Polo Lopez et al. (2020) [10,31], which stipulates that integrating RES in heritage buildings can play a fundamental role in net-zero energy use targets for heritage buildings. However, in this work, a detailed structural analysis of the selected buildings is not investigated. This analysis is highly recommended when it comes to heritage buildings to accurately

check the weights of the proposed newly added systems—VRF HVAC system, PV, and SWHs—and the ability to add them to heritage buildings. More importantly, this study does not address the analysis of the economic aspect to optimally select cost-effective materials and technologies, e.g., VRF HVAC system. Moreover, feasibility studies of the annual GHG reduction in terms of CO₂ by applying RES should be investigated.

4.3. Study Implications and Future Studies

This study investigates the potentiality of heritage buildings to become energy neutral and supports their transition towards clean energy utilization in hot, dry climates. This will help to set a comprehensive tool for making decisions regarding the most effective retrofitting procedures. A heritage residential building stock of Khedivial Cairo acted as a case study area with a microscale analysis on real reference buildings. This area was selected due to its significant cultural value and for the possibility of expanding this concept to similar heritage residential building stock in North Africa in particular, and hot, dry climates in general. Future work may focus on addressing urban analysis to achieve sustainability goals. For example, investigation of life cycle analysis (LCA) embodied energy, carbon footprint, waste management, etc., to indicate the risk based on this life cycle approach.

5. Conclusions

In this work, we developed an integrated retrofitting methodology that balanced multi-performance targets in historic districts in hot climates. Moreover, we identified the most effective retrofitting solutions in terms of three performance targets: indoor thermal comfort, the potential for zero energy use, and compatibility with cultural values. The central questions revolved around how heritage buildings can transform to become energy neutral in such a climate, and what optimal scenarios can achieve nearly-zero energy use while keeping their cultural values. To find answers, an integrated retrofitting methodology was proposed, and for its validation, it was applied in a case study with a microscale analysis of real buildings. Three reference buildings representing the most dominant building typologies in Khedivial Cairo were selected. The proposed methodology included the following four-phase process: (1) selecting reference buildings, (2) evaluating the building envelope and energy performance, (3) determining cultural value restrictions and proposing energy retrofitting strategies, and (4) evaluating annual improvements and the compatibility of energy retrofitting strategies with local legislations to define the multi-objective optimization case. The main findings of this study revealed that the proposed retrofitting methodology is a useful tool, as shown in the results of its application on three reference buildings in Khedivial Cairo. The best outcome of this application is a proposal of the “nearly-ZEB case” scenario, which is highly compatible with the conservation of cultural values. However, this study is limited by focusing on three performance aspects: building energy performance, achieving indoor thermal comfort, and the conservation of cultural values. It does not address both the economical and structural feasibility of applying the proposed scenarios. For future research, further studies on embodied energy and the carbon footprint of heritage residential building stocks should be considered.

Author Contributions: Conceptualization, H.S.S.I., A.Z.K., S.A. and Y.S.; methodology, H.S.S.I., A.Z.K. and S.A.; software, H.S.S.I.; field surveys, H.S.S.I.; resources, H.S.S.I., A.Z.K. and Y.S.; data curation, H.S.S.I. and S.A.; writing—original draft preparation, H.S.S.I.; writing—review and editing, H.S.S.I., A.Z.K., S.A. and Y.S.; visualization, H.S.S.I.; validation H.S.S.I. and S.A.; supervision, A.Z.K., S.A. and Y.S. All authors have read and agreed to the published version of the manuscript.

Funding: This research received no external funding.

Institutional Review Board Statement: The institutional review board of FUE, Egypt, and ULB, Belgium, provided consent for this research and had no objections.

Informed Consent Statement: The residents of the buildings were informed regarding the research, survey, interview, and data collection. The authors can provide the essential data upon request, considering privacy and data protection.

Data Availability Statement: The data presented in this study are available on request from the corresponding author.

Acknowledgments: The authors acknowledge the Future University in Egypt (FUE) for providing the necessary funds and resources to complete the Ph.D. degree of the first author.

Conflicts of Interest: The authors declare no conflict of interest. The funders had no role in the study's design; in the collection, analysis, or interpretation of the data; in the writing of the manuscript; or in the decision to publish the results.

Appendix A. Thermal Properties of Materials Used in the Reference Buildings in Terms of Conductivity, Specific Heat Capacity, and Density

Table A1. Thermal properties of the building elements of the base case buildings 7 and 9.

No.	Building Element	Outside to Inside	Composition	Thickness (m)	Conductivity * (W/m · k)	Specific Heat Capacity * (J/kg · k)	Density * (kg/m ³)
				<i>t</i>	λ	c_p	<i>D</i>
1	Exterior wall	Layer 1	Limestone, soft	0.02	0.93	900	1650
		Layer 2	Cement mortar	0.02	0.9	896	1570
		Layer 3	Burnt-brick	0.25	0.85	480	1500
		Layer 4	Cement plaster	0.02	0.72	840	1760
2	Internal wall	Layer 1	Cement plaster	0.02	0.72	840	1760
		Layer 2	Burnt-brick	0.12	0.85	480	1500
		Layer 3	Cement plaster	0.02	0.72	840	1760
3	Internal floor	Layer 1	Mosaico tiles	0.02	1.6	840	2450
		Layer 2	Cement mortar	0.02	0.9	896	1570
		Layer 3	Sand	0.06	0.33	800	1520
		Layer 4	Reinforced concrete slab	0.15	1.9	840	2300
		Layer 5	Cement plaster	0.02	0.72	840	1760
4	Ground floor	Layer 1	Mosaico tiles	0.02	1.6	840	2450
		Layer 2	Cement mortar	0.02	0.9	896	1570
		Layer 3	Sand	0.06	0.33	800	1520
		Layer 4	Concrete, cast, no fines	0.3	1.44	840	2460
5	Roof	Layer 1	Roofing tiles	0.02	1.5	1000	2100
		Layer 2	Cement mortar	0.02	0.9	896	1570
		Layer 3	Sand	0.06	0.33	800	1520
		Layer 4	Reinforced concrete slab	0.15	1.9	840	2300
		Layer 5	Cement plaster	0.02	0.72	840	1760

* Most of the thermal properties of materials are extracted from the Egyptian guidelines for specifications of building construction materials [12,35].

Table A2. Thermal properties of the building elements of the base case building 8.

No.	Building Element	Outside to Inside	Composition	Thickness (m)	Conductivity * (W/m · k)	Specific Heat Capacity * (J/kg · k)	Density * (kg/m ³)
				t	λ	c_p	D
1	Exterior wall	Layer 1	Limestone hard	0.05	0.7	1000	2200
		Layer 2	Cement mortar	0.02	0.9	896	1570
		Layer 3	Brick	0.5	0.85	480	1500
		Layer 4	Cement plaster	0.02	0.72	840	1760
2	Internal wall	Layer 1	Cement plaster	0.02	0.72	840	1760
		Layer 2	Brick	0.5	0.85	480	1500
		Layer 3	Cement plaster	0.02	0.72	840	1760
3	Internal floor	Layer 1	Marble	0.04	2.77	802	2600
		Layer 2	Cement mortar	0.02	0.9	896	1570
		Layer 3	Sand	0.06	0.33	800	1520
		Layer 4	Reinforced concrete slab	0.15	1.9	840	2300
		Layer 5	Cement plaster	0.02	0.72	840	1760
4	Ground floor	Layer 1	Marble	0.04	2.77	802	2600
		Layer 2	Cement mortar	0.02	0.9	896	1570
		Layer 3	Sand	0.06	0.33	800	1520
		Layer 4	Concrete, cast, no fines	0.3	1.44	840	2460
5	Roof	Layer 1	Roofing tiles	0.02	0.5	1000	2100
		Layer 2	Cement mortar	0.02	0.9	896	1570
		Layer 3	Sand	0.06	0.33	800	1520
		Layer 4	Concrete, cast, no fines	0.07	1.44	840	2460
		Layer 5	Reinforced concrete slab	0.15	1.9	840	2300
		Layer 6	Cement plaster	0.02	0.72	840	1760

Appendix A.1. Schedules

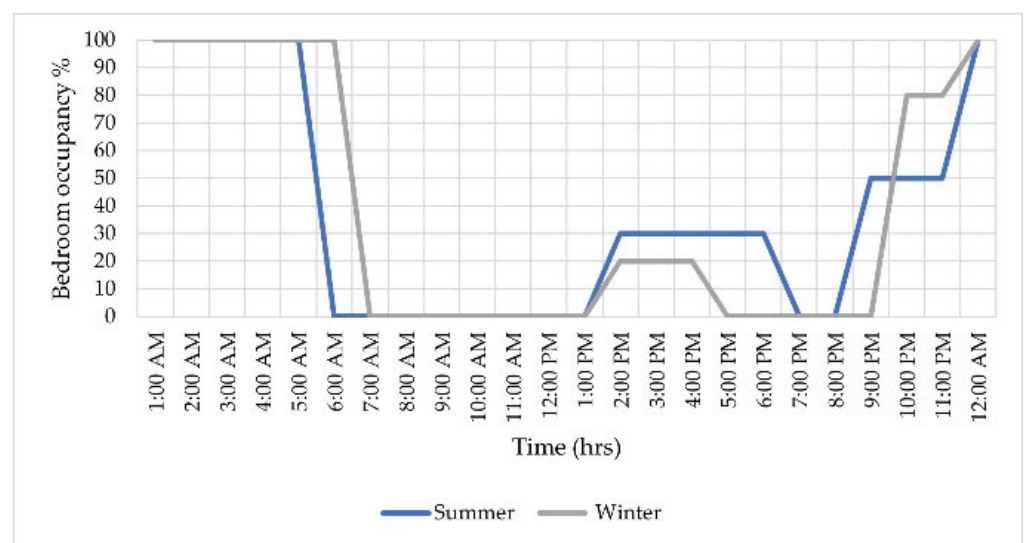


Figure A1. Bedroom occupancy schedule.

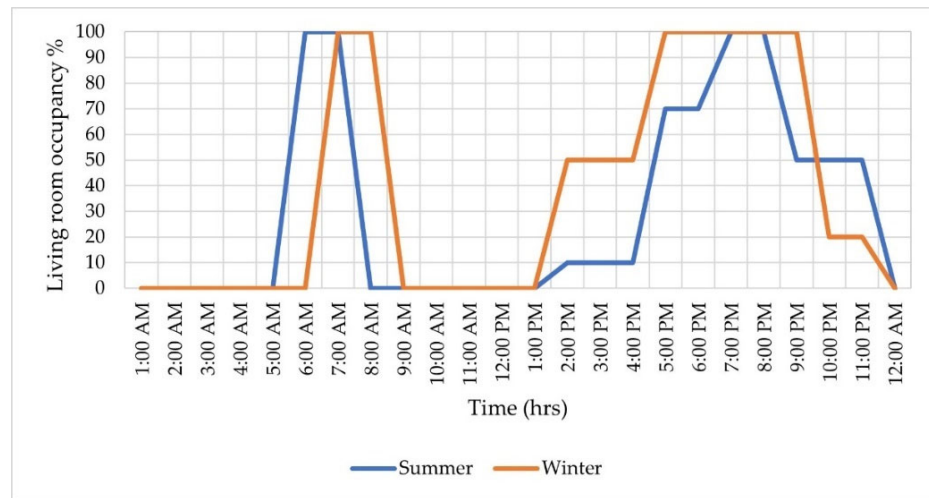


Figure A2. Living room occupancy schedule.

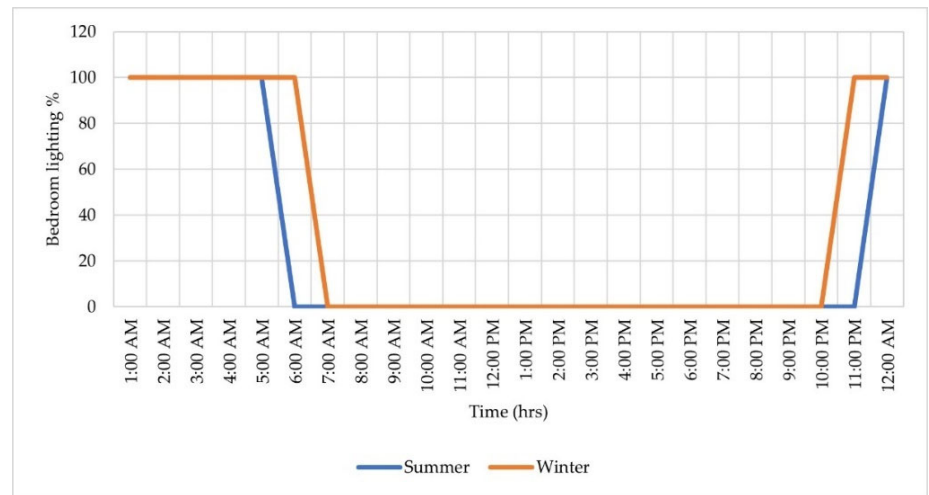


Figure A3. Bedroom lighting schedule.

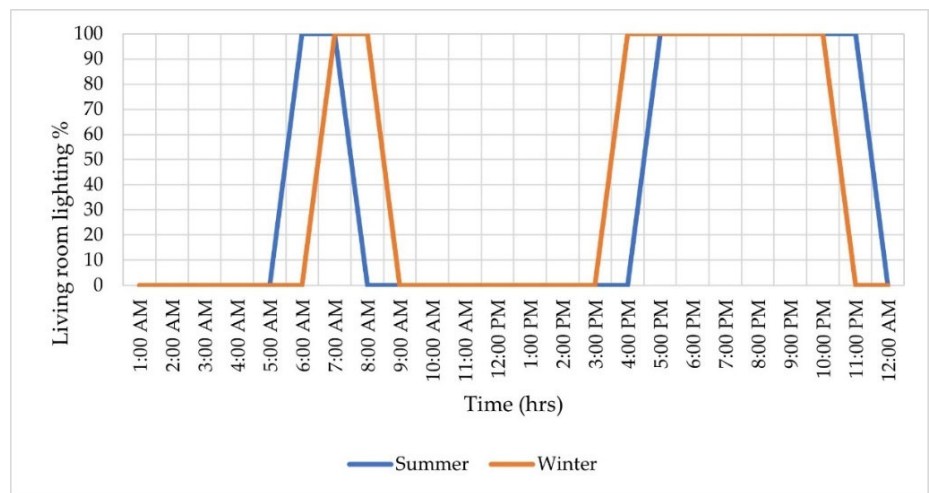


Figure A4. Living room lighting schedule.

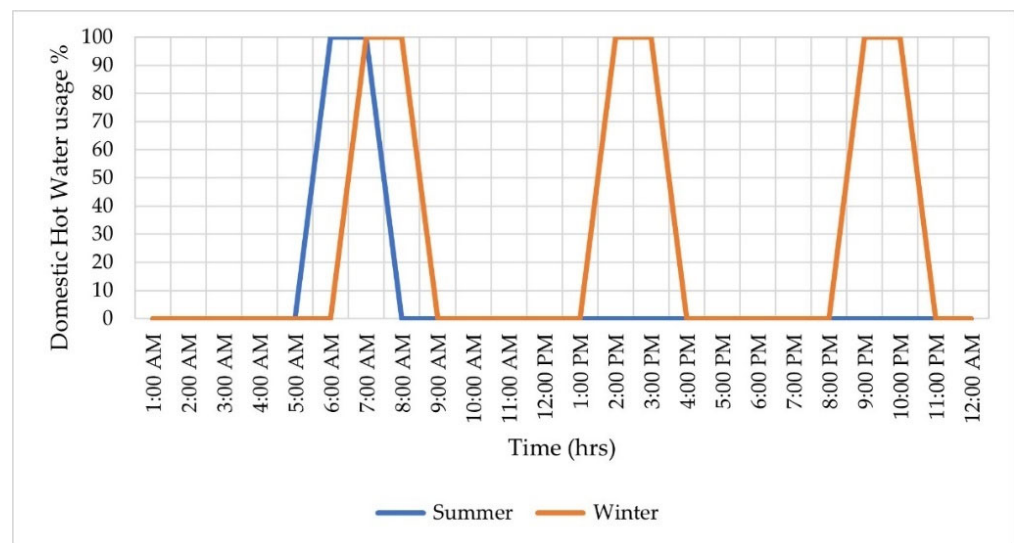


Figure A5. Domestic hot water schedule.

Appendix A.2. Linear Regression Analysis of Calibration of the Simulation Models for Winter

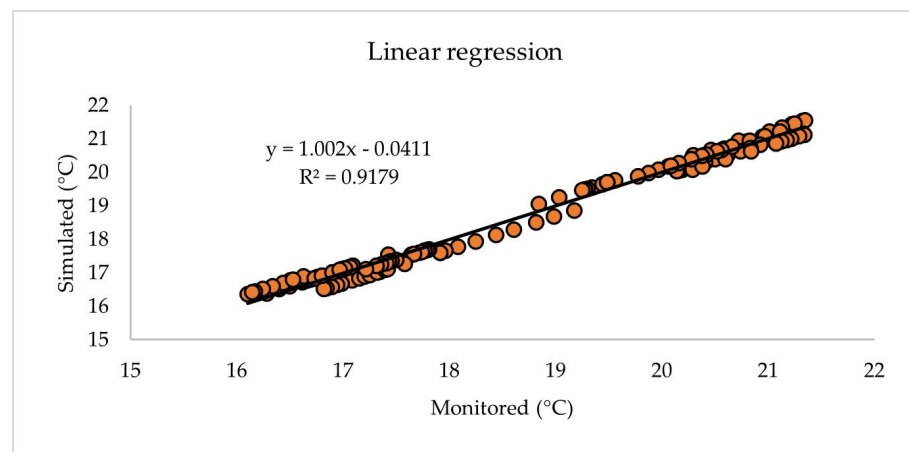


Figure A6. Reference building 7.

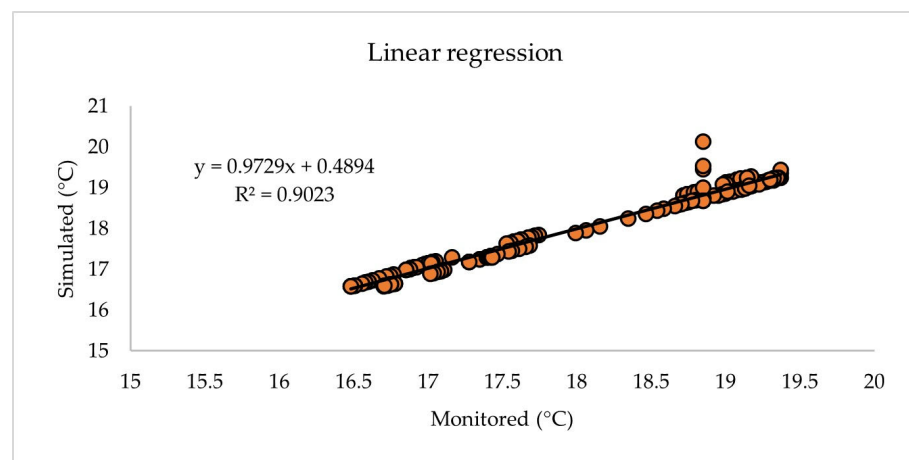


Figure A7. Reference building 8.

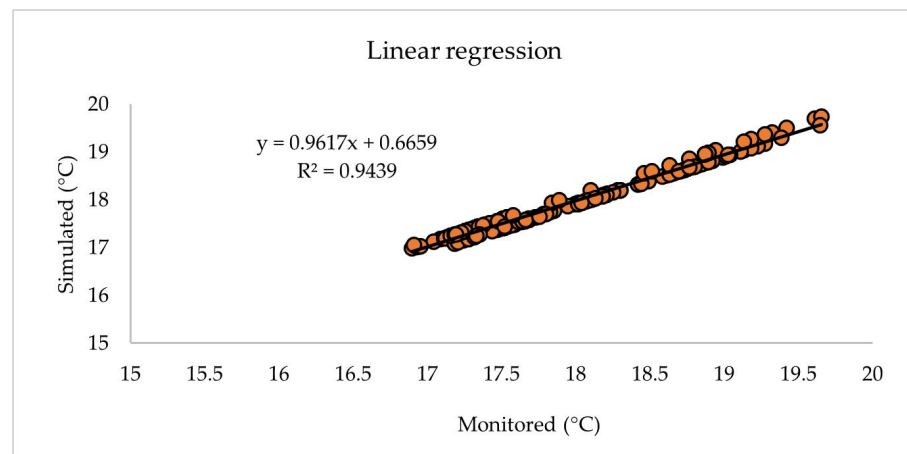


Figure A8. Reference building 9.

Appendix B. Equations Used to Calculate the Solar Fraction for Solar Water Heaters SWHs

Equations (A1) and (A2): Equation (A1) is used to calculate energy collected per unit collector area for glazed solar water heaters SWHs, whereas Equation (A2) is used for evacuated ones, based on [79,80,85–88].

$$Q_{\text{coll}} = F_R(\tau\alpha)G - F_R U_L \Delta T \quad (\text{A1})$$

$$Q_{\text{coll}} = (F_R \alpha) \left((G) + \left(\frac{\varepsilon}{\alpha} \right) L \right) - F_R U_L \Delta T \quad (\text{A2})$$

Equations (A3)–(A5): The f-Chart model is presented as a function of two dimensionless parameters X and Y, based on [79,80,85–88].

$$X = \frac{A_c F_R U_L (T_{\text{ref}} - T_a)}{L} \quad (\text{A3})$$

$$Y = \frac{A_c F_R (\tau\alpha) H_T N}{L} \quad (\text{A4})$$

$$f = 1.029Y - 0.065X - 0.245Y^2 + 0.0018X^2 + 0.215Y^2 \quad (\text{A5})$$

Q_{coll} = energy collected per unit collector area per unit time;

F_R = overall collector heat removal efficiency factor;

$(\tau\alpha)$ = monthly average transmittance–absorptance product;

τ = transmittance of the product cover;

α = shortwave absorptivity of the absorber;

G (W/m^2) = global incident solar radiation on the collector;

U_L ($\text{W}/\text{m}^2 \cdot ^\circ\text{C}$) = overall heat loss coefficient of collector;

ΔT ($^\circ\text{C}$) = difference between the temperature of working fluid entering and leaving the collector;

A_c (m^2) = collector area;

T_a ($^\circ\text{C}$) = monthly average ambient temperature;

T_{ref} (100°C) = empirical reference temperature;

L (J) = monthly total heating load for hot water;

H_T (J/m^2) = monthly average daily radiation incident on collector;

N = number of days in month;

F = solar fraction of total monthly load provided by SWHs.

References

- International Energy Agency (IEA). Net Zero by 2050 A Roadmap for the Global Energy. Available online: <https://www.iea.org/data-and-statistics/data-product/net-zero-by-2050-scenario> (accessed on 25 May 2021).
- Gremmelspacher, J.M.; Pizarro, R.C.; van Jaarsveld, M.; Davidsson, H.; Johansson, D. Historical building renovation and PV optimisation towards NetZEB in Sweden. *Sol. Energy* **2021**, *223*, 248–260. [\[CrossRef\]](#)
- Miljödepartementet, Klimatpolitiska Handlingsplanen; Technical Report: 2019; Ministry of the Environment: Stockholm, Sweden, 2019.
- Lee, J.; Shepley, M.M.; Choi, J. Exploring the effects of a building retrofit to improve energy performance and sustainability: A case study of Korean public buildings. *J. Build. Eng.* **2019**, *25*, 100822. [\[CrossRef\]](#)
- Fouseki, K.; Newton, D.; Camacho, K.S.M.; Nandi, S.; Koukou, T. Energy Efficiency, Thermal Comfort, and Heritage Conservation in Residential Historic Buildings as Dynamic and Systemic Socio-Cultural Practices. *Atmosphere* **2020**, *11*, 604. [\[CrossRef\]](#)
- Ali, U.; Shamsi, M.H.; Bohacek, M.; Hoare, C.; Purcell, K.; Mangina, E.; O'Donnell, J. A data-driven approach to optimize urban scale energy retrofit decisions for residential buildings. *Appl. Energy* **2020**, *267*, 114861. [\[CrossRef\]](#)
- Lidelöw, S.; Örn, T.; Luciani, A.; Rizzo, A. Energy-efficiency measures for heritage buildings: A literature review. *Sustain. Cities Soc.* **2019**, *45*, 231–242. [\[CrossRef\]](#)
- Cho, H.M.; Yun, B.Y.; Yang, S.; Wi, S.; Chang, S.J.; Kim, S. Optimal energy retrofit plan for conservation and sustainable use of historic campus building: Case of cultural property building. *Appl. Energy* **2020**, *275*, 115313. [\[CrossRef\]](#)
- Energy in Buildings and Communities Programme (EBC). EBC ANNEX 76-SHC TASK 59, *Deep Renovation of Historic Buildings Towards Lowest Possible Energy Demand and CO₂ Emissions*; Executive Committee Support Services Unit, AECOM: London, UK, 2019.
- Lopez, C.P.; Lucchi, E.; Franco, G. Acceptance of Building Integrated Photovoltaic (BIPV) in Heritage Buildings and Landscapes: Potentials, Barrier and Assessment Criteria. In Proceedings of the Rehabend Conference, Construction Pathology, Rehabilitation Technology and Heritage Management, Granada, Spain, 24–27 March 2020.
- Martinez-Molina, A.; Tort-Ausina, I.; Cho, S.; Vivancos, J.-L. Energy efficiency and thermal comfort in historic buildings: A review. *Renew. Sustain. Energy Rev.* **2016**, *61*, 70–85. [\[CrossRef\]](#)
- Ibrahim, H.S.S.; Khan, A.Z.; Mahar, W.A.; Attia, S.; Serag, Y. Assessment of Passive Retrofitting Scenarios in Heritage Residential Buildings in Hot, Dry Climates. *Energies* **2021**, *14*, 3359. [\[CrossRef\]](#)
- Lelieveld, J.; Proestos, Y.; Hadjinicolaou, P.; Tanarhte, M.; Tyrllis, E.; Zittis, G. Strongly increasing heat extremes in the Middle East and North Africa (MENA) in the 21st century. *Clim. Chang.* **2016**, *137*, 245–260. [\[CrossRef\]](#)
- Lange, M.A. Impacts of climate change on the Eastern Mediterranean and the Middle East and North Africa region and the water–energy nexus. *Atmosphere* **2019**, *10*, 455. [\[CrossRef\]](#)
- Salameh, T.; Tawalbeh, M.; Juaidi, A.; Abdallah, R.; Hamid, A.-K. A novel three-dimensional numerical model for PV/T water system in hot climate region. *Renew. Energy* **2021**, *164*, 1320–1333. [\[CrossRef\]](#)
- Salameh, T.; Ghenai, C.; Merabet, A.; Alkasrawi, M. Techno-economical optimization of an integrated stand-alone hybrid solar PV tracking and diesel generator power system in Khorfakkan, United Arab Emirates. *Energy* **2020**, *190*, 116475. [\[CrossRef\]](#)
- Salameh, T.; Assad, M.E.; Tawalbeh, M.; Ghenai, C.; Merabet, A.; Öztıp, H.F. Analysis of cooling load on commercial building in UAE climate using building integrated photovoltaic façade system. *Sol. Energy* **2020**, *199*, 617–629. [\[CrossRef\]](#)
- International Bank for Reconstruction and Development/The World Bank. *Report No: ACS22504, Egypt Energy Efficiency Implementation, Energy Efficiency and Rooftop Solar PV Opportunities: Report Summary*; International Bank for Reconstruction and Development/The World Bank: Cairo, Egypt, 2017.
- Egyptian Electricity Holding Company (EEHC). *Annual Report 2018/2019*; Ministry of Electricity & Renewable Energy: Cairo, Egypt, 2020.
- Attia, S.; Evrard, A.; Gratia, E. Development of benchmark models for the Egyptian residential buildings sector. *Appl. Energy* **2012**, *94*, 270–284. [\[CrossRef\]](#)
- Abdallah, L. Egypt's nationally determined contributions to Paris agreement: Review and recommendations. *Int. J. Ind. Sustain. Dev.* **2020**, *1*, 49–59. [\[CrossRef\]](#)
- Central Agency for Public Mobilization and Statistics (CAPMAS). *Housing and Establishment Census 2017*; CAPMAS: Egypt, Cairo, 2019.
- Berggren, B. Evaluating Energy Efficient Buildings: Energy- and Moisture Performance Considering Future Climate Change. Doctoral Thesis, Lund University, Lund, Sweden, 2019.
- Ibrahim, H.S.S.; Khan, A.Z.; Attia, S.; Serag, Y. Classification of Heritage Residential Building Stock and Defining Sustainable Retrofitting Scenarios in Khedivial Cairo. *Sustainability* **2021**, *13*, 880. [\[CrossRef\]](#)
- Ibrahim, H.S.S.; Khan, A.Z.; Ali, M.A.M.; Serag, Y. Evaluation of a Retrofitted Heritage Building in Downtown Cairo as a Best-Practice Example. In Proceedings of the SBE21 Sustainable Built Heritage, Renovating Historic Buildings for a Low-Carbon Built, Bolzano, Italy, 14–16 April 2021.
- Webb, A.L. Energy retrofits in historic and traditional buildings: A review of problems and methods. *Renew. Sustain. Energy Rev.* **2017**, *77*, 748–759. [\[CrossRef\]](#)
- Kotteck, M.; Jürgen, G.; Christoph, B.; Bruno, R.; Franz, R. World map of the Köppen-Geiger climate classification updated. *Meteorol. Zeitschrift.* **2006**, *15*, 259–263. [\[CrossRef\]](#)
- Sahin, C.D.; Arsan, Z.D.; Tunçoku, S.S.; Broström, T.; Akkurt, G.G. A transdisciplinary approach on the energy efficient retrofitting of a historic building in the Aegean Region of Turkey. *Energy Build.* **2015**, *96*, 128–139. [\[CrossRef\]](#)

29. Güleroğlu, S. K.; Karagüler, M.E.; Kahraman, I.; Umdü, E.S. Methodological approach for performance assessment of historical buildings based on seismic, energy and cost performance: A Mediterranean case. *J. Build. Eng.* **2020**, *31*, 101372. [CrossRef]
30. Bellia, L.; Alfano, F.R.; Giordano, J.; Ianniello, E.; Riccio, G. Energy requalification of a historical building: A case study. *Energy Build.* **2015**, *95*, 184–189. [CrossRef]
31. Lucchi, E.; Lopez, C.P.S.; Franco, G. A conceptual framework on the integration of solar energy systems in heritage sites and buildings. *IOP Conf. Ser. Mater. Sci. Eng.* **2020**, *949*, 012113. [CrossRef]
32. Attia, S.; De Herde, A.; Gratia, E.; Hensen, J.L. Achieving informed decision-making for net zero energy buildings design using building performance simulation tools. *Build. Simul.* **2013**, *16*, 3–21. [CrossRef]
33. Fahmy, M.; Mahmoud, S.; Elwy, I.; Mahmoud, H. A Review and Insights for Eleven Years of Urban Microclimate Research Towards a New Egyptian ERA of Low Carbon, Comfortable and Energy-Efficient Housing Typologies. *Atmosphere* **2020**, *11*, 236. [CrossRef]
34. Housing and Building National Research Center (HBRC). *The Egyptian Code for Energy Efficiency Improvement in Buildings Part 1 (ECP 306–2005)*; Ministry of Housing, Utilities & Urban Communities: Cairo, Egypt, 2006. (In Arabic)
35. Housing and Building National Research Center (HBRC). *Specifications of Thermal Insulation Work Items*; Ministry of Housing, Utilities & Urban Communities: Cairo, Egypt, 2007.
36. Egyptian Prime Minister, *Egyptian Law No. 144 of 2006, Regulation of the Demolition of Unthreatened Buildings and Constructions and the Conservation of the Architectural Heritage*; The Egyptian Gazette (Al-Waqa' al-Misriyya): Cairo, Egypt, 2006. (In Arabic)
37. Attia, S.; De Herde, A. Impact and potential of community scale low-energy retrofit: Case study in Cairo. In Proceedings of the 3rd CIB International Conference on Smart and Sustainable Built Environments, Delft, The Netherlands, 15–19 June 2009.
38. General Meteorological Authority. *Statistical Yearbook, Geography & Climate*; General Meteorological Authority: Cairo, Egypt, 2016.
39. Mostafa, A.N.; Wheida, A.; El Nazer, M.; Adel, M.; El Leithy, L.; Siour, G.; Coman, A.; Borbon, A.; Magdy, A.W.; Omar, M.; et al. Past (1950–2017) and future (–2100) temperature and precipitation trends in Egypt. *Weather Clim. Extrem.* **2019**, *26*, 100225. [CrossRef]
40. Weather Data/EnergyPlus. Available online: <https://energyplus.net/weather> (accessed on 26 April 2021).
41. BizEE Degree Days, Weather Data for Energy Saving. Available online: <https://www.degreedays.net> (accessed on 26 April 2021).
42. Setyantho, G.R.; Park, H.; Chang, S. Multi-Criteria Performance Assessment for Semi-Transparent Photovoltaic Windows in Different Climate Contexts. *Sustainability* **2021**, *13*, 2198. [CrossRef]
43. Photovoltaic Geographical Information System, European Commission EU. Available online: <https://re.jrc.ec.europa.eu> (accessed on 1 June 2021).
44. GEO-CRADLE. *The Solar Atlas of Egypt, The European Union's Horizon 2020 Research and Innovation Programme*; European Commission: Brussels, Belgium, 2013.
45. RETScreen® Software Online Manual. Solar Water Heating Project Model. RET Screen International Clean Energy Decision Support Centre. 2005. Available online: www.retscreen.net (accessed on 5 July 2021).
46. Mahar, W.A.; Verbeeck, M. K.S.G.; Attia, S. An investigation of thermal comfort of houses in dry and semi-arid climates of Quetta, Pakistan. *Sustainability* **2019**, *11*, 5203. [CrossRef]
47. Semahi, S.; Noureddine, Z.; Manoj, K.S.; Attia, S. Comparative bioclimatic approach for comfort and passive heating and cooling strategies in Algeria. *Build. Environ.* **2019**, *161*, 106271. [CrossRef]
48. Attia, S.; Carlucci, S. Impact of different thermal comfort models on zero energy residential buildings in hot climate. *Energy Build.* **2015**, *102*, 117–128. [CrossRef]
49. Attia, S.; Hamdy, M.; Ezzeldin, S. Twenty-year tracking of lighting savings and power density in the residential sector. *Energy Build.* **2017**, *154*, 113–126. [CrossRef]
50. Attia, S.; De Herde, A. Strategic decision making for zero energy buildings in hot climates. In Proceedings of the EuroSun 2010, the 8th EuroSun Conference of ISES Europe, Graz, Austria, 28 September–1 October 2010.
51. Tabibian, S.; Ghavami, M. New HVAC system in restoration of historic buildings. *J. Nat. Sci. Sustain. Technol.* **2016**, *10*, 37.
52. Torregrosa-Jaime, B.; Martínez, P.J.; González, B.; Payá-Ballester, G. Modelling of a Variable Refrigerant Flow System in EnergyPlus for Building Energy Simulation in an Open Building Information Modelling Environment. *Energies* **2018**, *12*, 22. [CrossRef]
53. Thornton, B. *General Services Administration (Report)*; US Federal Government: Washington, DC, USA, 2012.
54. Afify, R. Designing VRF systems. *ASHRAE J.* **2008**, *50*, 52.
55. Aynur, T.N.; Hwang, Y.; Radermacher, R. Simulation comparison of VAV and VRF air conditioning systems in an existing building for the cooling season. *Energy Build.* **2009**, *41*, 1143–1150. [CrossRef]
56. Kim, D.; Cox, S.J.; Cho, H.; Im, P. Evaluation of energy savings potential of variable refrigerant flow (VRF) from variable air volume (VAV) in the U.S. climate locations. *Energy Rep.* **2017**, *3*, 85–93. [CrossRef]
57. Kani-Sanchez, C.; Richman, R. Incorporating variable refrigerant flow (VRF) heat pump systems in whole building energy simulation – Detailed case study using measured data. *J. Build. Eng.* **2017**, *12*, 314–324. [CrossRef]
58. Pelle, M.; Lucchi, E.; Maturi, L.; Astigarraga, A.; Causone, F. Coloured BIPV Technologies: Methodological and Experimental Assessment for Architecturally Sensitive Areas. *Energies* **2020**, *13*, 4506. [CrossRef]
59. Quintana, S.; Huang, P.; Saini, P.; Zhang, X. A preliminary techno-economic study of a building integrated photovoltaic (BIPV) system for a residential building cluster in Sweden by the integrated toolkit of BIM and PVSITES. *Intell. Build. Int.* **2021**, *13*, 51–69. [CrossRef]

60. Moschella, A.; Salemi, A.; Sanfilippo, G.; Detommaso, M.; Privitera, A. Historic buildings in Mediterranean area and solar thermal technologies: Architectural integration vs preservation criteria. *Energy Procedia* **2013**, *42*, 416–425. [CrossRef]
61. Gevorkian, P. *Solar Power in Building Design: The Engineer's Complete Design Resource*; McGraw-Hill Education: New York, NY, USA, 2008.
62. Kallioğlu, M.A.; Durmuş, A.; Karakaya, H.; Yılmaz, A. Empirical calculation of the optimal tilt angle for solar collectors in northern hemisphere. *Energy Sources Part A Recover. Util. Environ. Eff.* **2020**, *42*, 1335–1358. [CrossRef]
63. Darhmaoui, H.; Lahjouji, D. Latitude based model for tilt angle optimization for solar collectors in the Mediterranean region. *Energy Procedia* **2013**, *42*, 426–435. [CrossRef]
64. López, C.S.P.; Troia, F.; Nocera, F. Photovoltaic BIPV Systems and Architectural Heritage: New Balance between Conservation and Transformation. An Assessment Method for Heritage Values Compatibility and Energy Benefits of Interventions. *Sustainability* **2021**, *13*, 5107. [CrossRef]
65. Solar Panel Kits & Products. Longi Solar, Model ID (LR4-60HPH-360M). Available online: <https://www.solaris-shop.com> (accessed on 15 July 2021).
66. Bhargav, K.; Antony, S.M. A MPPT controller based Solar Power Generation using a Multilevel Inverter. *Int. J. Eng. Technol.* **2016**, *8*, 265–273.
67. Babes, B.; Boutaghane, A.; Hamouda, N. A novel nature-inspired maximum power point tracking (MPPT) controller based on ACO-ANN algorithm for photovoltaic (PV) system fed arc welding machines. *Neural Comput. Appl.* **2021**, 1–19. [CrossRef]
68. Fronius Primo 5.0-1 TL 5KW Inverter. Available online: <https://www.solaris-shop.com/fronius-primo-5-0-1-tl-5kw-inverter/> (accessed on 30 July 2021).
69. Horan, P.; Luther, M.B.; Li, H.X. Guidance on Implementing Renewable Energy Systems in Australian Homes. *Energies* **2021**, *14*, 2666. [CrossRef]
70. Salameh, T.; Abdelkareem, M.A.; Olabi, A.G.; Sayed, E.T.; Al-Chaderchi, M.; Rezk, H. Integrated standalone hybrid solar PV, fuel cell and diesel generator power system for battery or supercapacitor storage systems in Khorfakkan, United Arab Emirates. *Int. J. Hydrogen Energy* **2021**, *46*, 6014–6027. [CrossRef]
71. Hassan, A.S.; Cipcigan, L.; Jenkins, N. Optimal battery storage operation for PV systems with tariff incentives. *Appl. Energy* **2017**, *203*, 422–441. [CrossRef]
72. Muenzel, V.; Mareels, I.; De Hoog, J.; Vishwanath, A.; Kalyanaraman, S.; Gort, A. PV generation and demand mismatch: Evaluating the potential of residential storage. In Proceedings of the 2015 IEEE Power & Energy Society Innovative Smart Grid Technologies Conference (ISGT), Washington, DC, USA, 18–20 February 2015; pp. 1–5.
73. Weniger, J.; Tjaden, T.; Quaschnig, V. Sizing of Residential PV Battery Systems. *Energy Procedia* **2014**, *46*, 78–87. [CrossRef]
74. Aichhorn, A.; Greenleaf, M.; Li, H.; Zheng, J. A cost effective battery sizing strategy based on a detailed battery lifetime model and an economic energy management strategy. In Proceedings of the 2012 IEEE Power and Energy Society General Meeting, San Diego, CA, USA, 22–26 July 2012; pp. 1–8.
75. Xiao, H.; Pei, W.; Yang, Y.; Kong, L. Sizing of battery energy storage for micro-grid considering optimal operation management. In Proceedings of the 2014 International Conference on Power System Technology, Ghengdu, China, 20–22 October 2014; pp. 3162–3169.
76. Calculate Solar Array Size and Cost. Available online: http://sroeco.com/solar/calculate-solar-cost/what_size_solar_system_ (accessed on 14 June 2021).
77. Castro-Gutiérrez, J.; Celzard, A.; Fierro, V. Energy storage in supercapacitors: Focus on tannin-derived carbon electrodes. *Front. Mater.* **2020**, *7*, 217. [CrossRef]
78. Frattolillo, A.; Canale, L.; Ficco, G.; Mastino, C.C.; Dell'Isola, M. Potential for Building Façade-Integrated Solar Thermal Collectors in a Highly Urbanized Context. *Energies* **2020**, *13*, 5801. [CrossRef]
79. Raza, S.A.; Ahmad, S.S.; Ratlamwala, T.A.H.; Hussain, G.; Alkahtani, M. Techno-Economic Analysis of Glazed, Unglazed and Evacuated Tube Solar Water Heaters. *Energies* **2020**, *13*, 6261. [CrossRef]
80. Lima, J.B.A.; Prado, R.T.; Taborianski, V.M. Optimization of tank and flat-plate collector of solar water heating system for single-family households to assure economic efficiency through the TRNSYS program. *Renew. Energy* **2006**, *31*, 1581–1595. [CrossRef]
81. Çomaklı, K.; Çakır, U.; Kaya, M.; Bakirci, K. The relation of collector and storage tank size in solar heating systems. *Energy Convers. Manag.* **2012**, *63*, 112–117. [CrossRef]
82. Sizing The Solar Thermal Array. SunMaxx Solar. Available online: <https://www.sunmaxxsolar.com/architects-engineer-training/sizing-the-solar-thermal-array/> (accessed on 5 July 2021).
83. Calculation and Simulation of Solar Thermal Plants for Heating and Potable Water. Oventrop. Available online: <https://www.ventrop.com/en-GB/downloadsoftware/onlinecalculations/solarcalculation> (accessed on 5 July 2021).
84. RETScreen® International Software Product Database. RET Screen International Clean Energy Decision Support Centre. 2015. Available online: www.entscreen.net (accessed on 5 July 2021).
85. Duffie, J.A.; Beckman, W.A.; Worek, W.M. *Solar Engineering of Thermal Processes*, 2nd ed.; Wiley: Hoboken, NJ, USA; New York, NY, USA, 1991; p. 1919.
86. Hsieh, J.S. *Solar Energy Engineering*; Prentice-Hall, Inc.: Old Tappan, NJ, USA, 1986.

87. Yasin, A. Technical and Financial Assessment of Glazed and Evacuated Tubes Solar Collectors for Domestic Water Heating Application in Palestine. *An-Najah Univ. J. Res. A (Nat. Sci.)* **2017**, *31*, 151–172.
88. Liu, S.; Hao, B.; Chen, X.; Yao, C.; Zhou, W. Analysis on limitation of using solar fraction ratio as solar hot water system design and evaluation index. *Energy Procedia* **2015**, *70*, 353–360. [[CrossRef](#)]
89. Guide Specifications. Aquatherm Industries. Available online: <http://aquathermsolar.com/specs/> (accessed on 15 June 2021).
90. SOLTOP Schuppisser. 2016. Available online: <https://www.soltop.ch/> (accessed on 15 June 2021).
91. Shangdong Linuo Paradigma. Available online: <http://www.linuo-ritter-international.com/> (accessed on 15 June 2021).
92. Abd-Ur-Rehman, H.M.; Al-Sulaiman, F.A. Techno-Economic Evaluation of Different Types of Solar Collectors for Water Heating Application in Domestic Sector of Saudi Arabia. In Proceedings of the 2014 5th International Renewable Energy Congress (IREC), Hammamet, Tunisia, 25–27 March 2014; pp. 1–6.
93. Khatri, R.; Joshi, A. Energy performance comparison of inverter based variable refrigerant flow unitary AC with constant volume unitary AC. *Energy Procedia* **2017**, *109*, 18–26. [[CrossRef](#)]